Engineering xxx (xxxx) xxx

Contents lists available at ScienceDirect

Engineering

journal homepage: www.elsevier.com/locate/eng

Research
Clean Power Technology—Review

Advances in Triboelectric Nanogenerators for Blue Energy Harvesting and Marine Environmental Monitoring

Yang Jiang [a,b,#], Xi Liang [a,b,#], Tao Jiang [a,b,*], Zhong Lin Wang [a,c,*]

[a] CAS Center for Excellence in Nanoscience, Beijing Key Laboratory of Micro–Nano Energy and Sensors, Beijing Institute of Nanoenergy and Nanosystems, Chinese Academy of Sciences, Beijing 101400, China
[b] School of Nanoscience and Technology, University of Chinese Academy of Sciences, Beijing 100049, China
[c] Georgia Institute of Technology, Atlanta, GA 30332, USA

ARTICLE INFO

Article history:
Received 11 February 2023
Revised 18 May 2023
Accepted 31 May 2023
Available online xxxx

Keywords:
Triboelectric nanogenerator (TENG)
TENG networks
Blue energy
Energy harvesting
Ocean sensors

ABSTRACT

Blue energy, which includes rainfall, tidal current, wave, and water-flow energy, is a promising renewable resource, although its exploitation is limited by current technologies and thus remains low. This form of energy is mainly harvested by electromagnetic generators (EMGs), which generate electricity via Lorenz force-driven electron flows. Triboelectric nanogenerators (TENGs) and TENG networks exhibit superiority over EMGs in low-frequency and high-entropy energy harvesting as a new approach for blue energy harvesting. A TENG produces electrical outputs by adopting the mechanism of Maxwell's displacement current. To date, a series of research efforts have been made to optimize the structure and performance of TENGs for effective blue energy harvesting and marine environmental applications. Despite the great progress that has been achieved in the use of TENGs in this context so far, continuous exploration is required in energy conversion, device durability, power management, and environmental applications. This review reports on advances in TENGs for blue energy harvesting and marine environmental monitoring. It introduces the theoretical foundations of TENGs and discusses advanced TENG prototypes for blue energy harvesting, including TENG structures that function in freestanding and contact-separation modes. Performance enhancement strategies for TENGs intended for blue energy harvesting are also summarized. Finally, marine environmental applications of TENGs based on blue energy harvesting are discussed.

1. Introduction

The ocean accounts for 70.8% of the earth's total area. In addition to making shipping possible, the ocean provides humanity with aquatic products, rich mineral deposits, and huge amounts of blue energy [1–5]. The term "new ocean energy" refers to the renewable energy that can be obtained from seawater, including tidal, wave, ocean current, temperature-difference, and salinity-gradient energy [3,6–11]. As it is renewable and less harmful to the environment than traditional energy sources, ocean energy has attracted extensive attention and has been estimated to have the potential to provide 77.6 billion kilowatts. Carbon neutrality requires a balance to be achieved between carbon emissions and absorptions [1,12–16]. One of the most effective methods for reaching carbon neutrality is to develop clean energy, such as the enormous blue energy offered by the ocean [3,7,17–22]. The utilization of blue energy on a large scale will reduce carbon dioxide emissions, greatly alleviating the tension in the world's energy demands and changing the global energy structure [23–28]. The energy from the vertical and horizontal movements of sea surface waves and the pressure change of water in waves can be harvested and converted into electricity, in what is one of the key directions of ocean energy development. However, the technologies of wave energy harvesting and conversion are not mature enough for large-scale and commercial use, and an industrial chain has not yet been formed [29–32]. At present, water wave energy harvesting mainly uses electromagnetic generators (EMGs), which capture the water wave energy as mechanical energy and generate electricity via a transmission module [4,33–36]. However, EMG-based

* Corresponding authors.
E-mail addresses: jiangtao@binn.cas.cn (T. Jiang), zlwang@gatech.edu (Z.L. Wang).
# These authors contributed equally to this work.

https://doi.org/10.1016/j.eng.2023.05.023

Please cite this article as: Y. Jiang, X. Liang, T. Jiang et al., Advances in Triboelectric Nanogenerators for Blue Energy Harvesting and Marine Environmental Monitoring, Engineering, https://doi.org/10.1016/j.eng.2023.05.023

wave energy conversion devices have the drawbacks of high costs, difficult installation, easy erosion, low efficiency, and poor stability, which greatly hinder the large-scale development of blue energy.

The triboelectric nanogenerator (TENG), which is based on Maxwell's displacement current, was invented by Fan et al. [37] in 2012. The TENG is a novel technology that harvests mechanical energy to generate electricity by coupling triboelectrification with electrostatic induction [38–47]. Compared with the EMG, the TENG possesses the merits of light weight, high power density, cost effectiveness, easy fabrication, and versatile material choices [35,40,48–51]. The TENG and its network bring a new strategy for blue energy harvesting, as proposed by Wang et al. [38,40,44], Xu et al. [52], Yang et al. [53], Ying et al. [54], Zhang et al. [55], Zheng et al. [56], Zhou et al. [57], and Chen et al. [58] in 2014. Many units or arrayed prototypes have been designed to enhance the output performance of energy harvesting and conversion devices [59–64]. TENG devices can effectively harvest water energy and act as self-powered systems; thus, these devices have the advantages of being renewable and pollution-free, and can be applied to blue energy—a new energy source with strategic significance that urgently needs to be developed [27,35,65–72].

This article covers recent progress in blue energy harvesting and marine environmental monitoring by means of TENGs. The review mainly focuses on the theoretical foundations of TENGs and advanced TENG prototypes for blue energy harvesting, including the rolling-ball, cylindrical, swing, three-dimensional (3D) electrode, spring-assisted, mass-spring, and pendulum-like structures. Next, performance enhancement strategies for TENGs in blue energy harvesting are summarized. Finally, marine environmental applications of TENGs based on blue energy harvesting are discussed.

2. Theoretical foundations of TENGs

2.1. Fundamental physics mechanisms of TENGs

The TENG, which was first proposed by Wang in 2012, generates electricity through contact-separation between two different materials, based on the coupling effect of contact electrification (CE) and electrostatic induction. The theory of CE is based on the overlapped electron-cloud (OEC) model (called the Wang transition). In the OEC model, a shallowly bounded electron can move from one atom to another if the interatomic distance is shorter than the normal bonding length between the two atoms, due to the lowered potential barrier.

The output of the TENG originates from Maxwell's displacement current. To explain the contribution of electrostatic charges induced by CE in Maxwell's equations, Wang added an additional term $\boldsymbol{P}_S$ in the electric displacement vector $\boldsymbol{D}$ in 2017 [36,43], which is defined as follows:

$$\boldsymbol{D} = \varepsilon_0 \boldsymbol{E} + \boldsymbol{P} + \boldsymbol{P}_S \tag{1}$$

where $\boldsymbol{E}$ is the electric field, $\boldsymbol{P}$ is the polarization field due to the existence of an external electric field, $\boldsymbol{P}_S$ is polarization contributed by the presence of surface polarization changes induced from triboelectrification, and ε_0 is the vacuum permittivity.

By substituting Eq. (1) into Maxwell's equations and defining $\boldsymbol{D}' = \varepsilon_0 \boldsymbol{E} + \boldsymbol{P}$, the reformulated Maxwell's equations [73] become:

$$\nabla \cdot \boldsymbol{D}' = \rho_f - \nabla \cdot \boldsymbol{P}_S \tag{2}$$

$$\nabla \cdot \boldsymbol{B} = 0 \tag{3}$$

$$\nabla \times \boldsymbol{E} = -\frac{\partial \boldsymbol{B}}{\partial t} \tag{4}$$

$$\nabla \times \boldsymbol{H} = \boldsymbol{J} + \frac{\partial \boldsymbol{D}'}{\partial t} + \frac{\partial \boldsymbol{P}_S}{\partial t} \tag{5}$$

where $\boldsymbol{B}$ is the magnetic induction, $\boldsymbol{H}$ is the magnetic field, $\boldsymbol{J}$ is the free electric current density, $\frac{\partial \boldsymbol{D}'}{\partial t}$ is the displacement current due to the time-varying electric field and the electric field-induced medium polarization, and ρ_f is the free electric charge density. The second term, $\frac{\partial \boldsymbol{P}_S}{\partial t}$, represents the displacement current due to a non-electric field and an external strain field.

The conventional Maxwell equations are suited for media whose boundaries and volumes are fixed and stationary. However, in some cases of moving media and time-dependent configurations, these equations need to be expanded. Assuming the moving medium to be a rigid translation object with acceleration, Wang derived the expanded Maxwell equations from the integral forms of the four physics laws. If the relativistic effect is ignored, Maxwell's equations for a mechano-driven slow-moving media system are given by the following [74,75]:

$$\nabla \cdot \boldsymbol{D}' = \rho_f - \nabla \cdot \boldsymbol{P}_S \tag{6}$$

$$\nabla \cdot \boldsymbol{B} = 0 \tag{7}$$

$$\nabla \times (\boldsymbol{E} + \boldsymbol{v}_r \times \boldsymbol{B}) = -\frac{\partial}{\partial t}\boldsymbol{B} \tag{8}$$

$$\nabla \times [\boldsymbol{H} - \boldsymbol{v}_r \times (\boldsymbol{D}' + \boldsymbol{P}_S)] = \boldsymbol{J}_f + \rho_f \boldsymbol{v} + \frac{\partial}{\partial t}\boldsymbol{P}_S + \frac{\partial}{\partial t}\boldsymbol{D}' \tag{9}$$

where $\boldsymbol{v}$ is the moving velocity of the media as a whole in its chosen reference frame, such as the system translation velocity, and $\boldsymbol{v}_r$ is the relative movement velocity of the medium points in reference to this reference frame, such as the rotation. In the expanded Maxwell equations, the moving velocity must be much less than the speed of light in a vacuum, as the relativistic effect is ignored. These equations are the most comprehensive governing equations for TENGs, including the electromagnetic interaction, power generation, and their coupling; they are fundamental for dealing with the coupling among multiple mechano–electric–magnetic fields and their interaction.

2.2. Working modes of TENGs

Based on the coupling of CE and electrostatic induction, TENGs harvest energy from human motion, vibration, mechanical triggering, wind, flowing water, and so on. As shown in Fig. 1, TENGs are classified into four fundamental working modes: the vertical contact-separation mode, lateral sliding mode, single-electrode mode, and freestanding triboelectric-layer mode [38]. In the vertical contact-separation mode, after coming into physical contact with each other, the two triboelectric layers generate opposite charges on their surfaces (Fig. 1(a)). When the surfaces of the two triboelectric layers are separated, a potential drop is produced between the two electrodes to drive the flow of electrons through the connected load. As the gap vanishes, the potential disappears due to the vanishing of static charges, and the induced free charges flow back to achieve electrical equilibrium. This mode has advantages in terms of the practical applications of TENGs, including a high instantaneous power density and simple structure design.

As shown in Fig. 1(b), electricity is produced between the surfaces of the two triboelectric layers in the lateral sliding mode by means of periodic contact and separation. First, the two dielectric surfaces are oppositely charged after coming into physical contact, due to triboelectrification. Along the sliding direction, lateral polarization is generated, driving the flow of electrons between the top

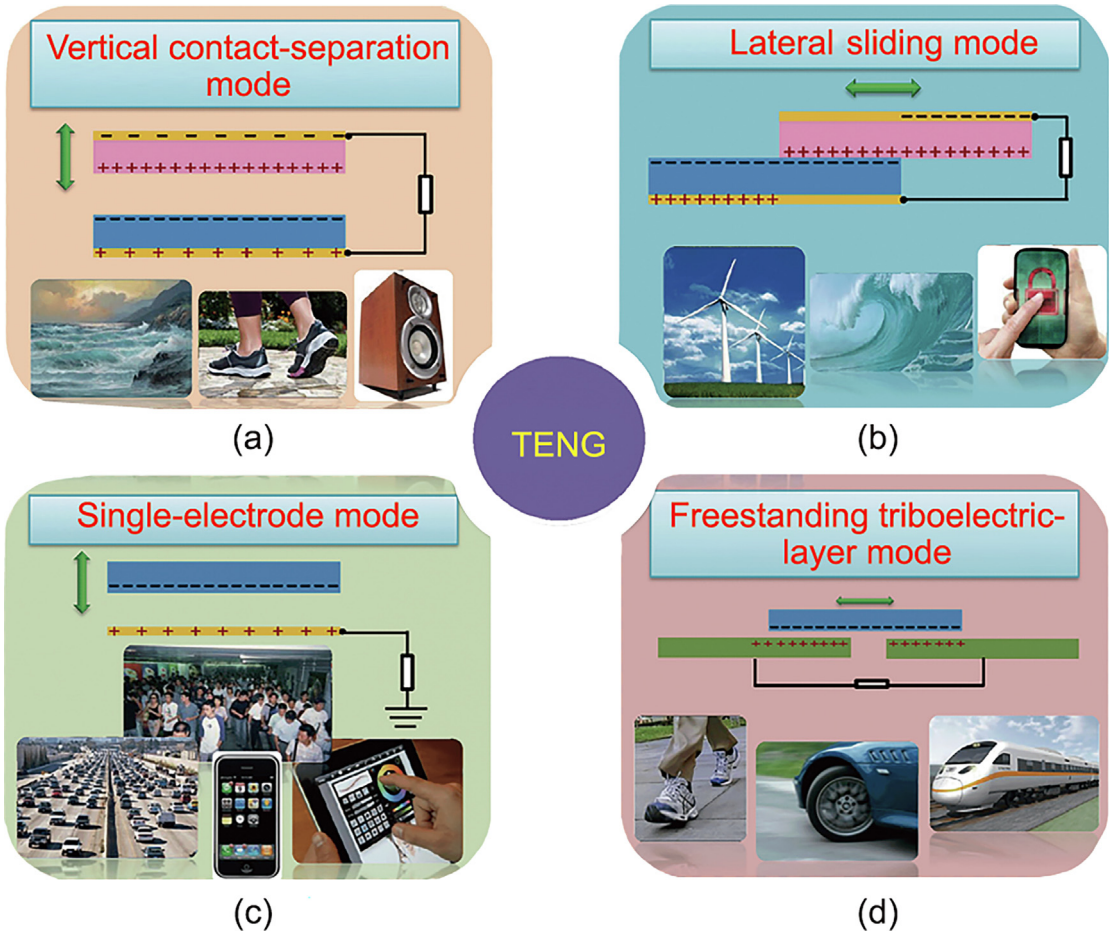

Fig. 1. The four fundamental modes of TENGs: (a) Vertical contact-separation mode; (b) lateral sliding mode; (c) single-electrode mode; (d) freestanding triboelectric-layer mode. Reproduced from Ref. [38] with permission.

and bottom electrodes to balance the electric field generated by the triboelectric charges. From the periodic sliding and closing, an alternating current (AC) output is generated. The lateral sliding mode generates more effective triboelectric charges than pure contact.

The vertical contact-separation and lateral sliding modes require two electrodes to be attached to the moving triboelectric layers. However, this is very inconvenient for practical applications, because connecting electrodes with mobile objects is difficult. In order to harvest energy in practical applications, the single-electrode TENG was introduced. As shown in Fig. 1(c), the single-electrode TENG has only one electrode, which is not connected to mobile objects. Due to the TENG's finite size, the approaching and departing of the top object will change the electrical field distribution, driving the electron flow between the bottom electrode and the ground to maintain a balanced potential. Because of the electrostatic screening effect, electrostatic-induced electron transfer is not the most effective form of transfer, but the charged object can move freely without any restriction. This advantage makes the single-electrodemode TENG suitable for acting as a self-powered active sensor to detect any electrically charged objects.

For the case of harvesting energy from a free-moving object, the freestanding triboelectric-layer mode has two symmetric stationary electrodes. The freestanding layer moves alternately to approach either electrode and induces a periodically reversed potential difference (Fig. 1(d)). Due to the lack of a screening effect, the freestanding triboelectric layer mode can transfer the triboelectric charges from the electrode to the freestanding layer. Therefore, the freestanding mode can harvest more effective energy than the single-electrode mode. Moreover, the triboelectric layer can achieve non-contact with the electrode layer during the sliding, which provides the advantage of improving the energy conversion efficiency and long-term stability by avoiding friction between the two surfaces.

2.3. Original idea of harvesting large-scale blue energy via TENGs

Based on the four fundamental modes above, a TENG can successfully harvest energy from the water surface, water waves, and water impacts on the shore. In 2014, Wang [38] proposed the idea of using 3D TENG networks to harvest large-scale ocean blue energy, because the water energy has a low frequency and is disordered (Fig. 2(a)). As shown in Fig. 2(b), a TENG network is made of millions of spherical TENG units connected in the form of a fishing net [40]. Given its low cost and simple structure, the network can be used for large-scale blue energy harvesting, and the total energy from gathering electric energy from all TENG units will be huge. The proposal of the TENG network brings new hope for utilizing and developing water energy and opens up a new way for humanity to obtain energy safely, continuously, and on a large scale.

The unmatched water frequency currently limits ocean wave energy harvesting with EMGs, making TENGs necessary. Table 1 [44,76] compares the technology of the TENG and the EMG. The EMG adopts the conduction current as its fundamental physical

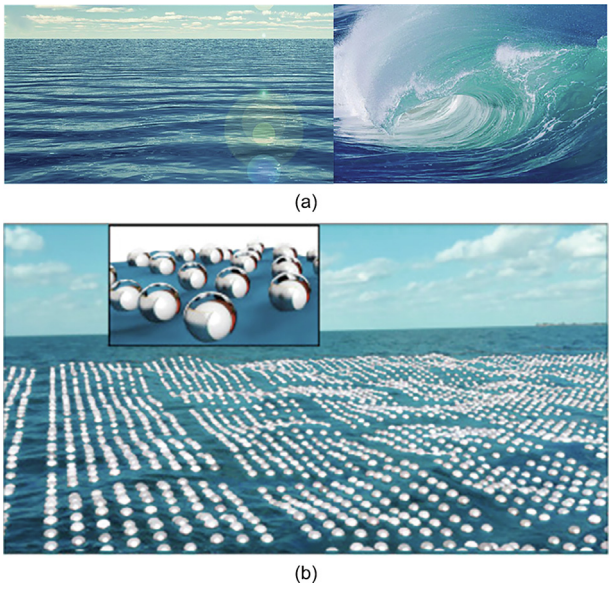

Fig. 2. (a) Schematic diagram of low-frequency and disordered blue energy; (b) the proposed idea of harvesting large-scale blue energy through TENG networks with millions of spherical TENG units. (a) Reproduced from Ref. [38] with permission, (b) reproduced from Ref. [40] with permission.

mechanism, whereas the TENG adopts Maxwell's displacement current. The EMG generates current through resistive free-electron conduction driven by the Lorentz force, while the TENG uses CE and electrostatic induction based on time-dependent electrostatic induction and a capacitive displacement current induced by the slight motion of bound static charges. The EMG is heavy, expensive, and easily corroded by seawater, but its durability is relatively high. In contrast, the TENG is lightweight and low in cost but presents the problems of high impedance and pulsed output. In addition, the TENG has multiple working modes, diverse material options, and numerous application fields.

A TENG used to collect wave energy does not use magnets and coils; instead, it uses lightweight and extremely cheap polymer materials to convert wave energy into electrical energy. The materials are all large-scale industrial raw materials, and the structure is simple and easy to form; thus, the production cost of a TENG is much lower than those of other power generation technologies, providing favorable conditions for its wide application. A TENG network does not occupy land area, and does not require dams to be built; it generates power day and night regardless of the weather and presents no potential strategic threat. TENG technology allows the devices to not only float on the water surface to collect wave energy but also capture the mechanical energy of the water flow. A TENG can collect mechanical energy from strong winds and waves and effectively manage small fluctuations.

3. Advanced TENG prototypes for blue energy harvesting

3.1. Freestanding-mode TENGs for water energy harvesting

3.1.1. Rolling-ball TENG

The rolling ball structure, which is made of a rolling ball inside a rocking spherical shell, is a typical structure for TENG-based water energy harvesting. Due to the low rolling friction, the rolling ball is simple and can scroll back and forth in the water, making it sensitive to tiny waves. Moreover, the sizes of the ball and shell in a rolling-ball TENG can be changed to achieve resonance with the water wave motions. The rolling-ball TENG also has the advantage of device durability, because there is no wire connected to the ball.

As shown in Fig. 3(a), Wang et al. [77] designed a rolling-structured, freestanding, fully enclosed TENG (RF-TENG) enclosing a rolling nylon ball with a Kapton film inside an enclosed rocking spherical shell. Driven by the wave vibration, the freestanding nylon ball can roll back and forth between the two electrodes to generate ACs across the external load. Compared with other rolling-structured TENGs in single-electrode and attached-electrode modes, this freestanding design has good charge transfer efficiency and high energy conversion efficiency, even under low-amplitude vibration. After theoretical simulations and experimental tests, the RF-TENG was demonstrated to achieve a maximum current of 1 μA and a peak power output of 10 mW under an external load in real water wave conditions.

Inspired by a wave power harvesting device known as the Edinburgh duck, a novel freestanding rolling mode TENG was designed in conjunction with an oscillating Salter's duck (Fig. 3(b)) [78]. The duck structure can harvest more than 80% of the mechanical energy in a wave under laboratory conditions, due to its efficient hydrodynamic structure. Within a wave, the front of the duck faces the wave and reflects only a small proportion of the wave energy; moreover, the duck structure does not transmit the waves downstream. The duck can rotate around an axis parallel to the incident waves, demonstrating high efficiency even under harsh conditions. A duck TENG system with three duck units has an instantaneous output power density of up to 1.366 $W{\cdot}m^{-2}$.

As shown in Fig. 3(c), Liu et al. [79] presented a torus-structured (TS)-TENG consisting of an inner ball and a torus shell. The inner ball rotates in the torus shell under the water waves, converting the water wave motion into electricity. The energy harvested by the TS-TENG can be stored for persistently powering electronics and charging a battery or capacitor. The TS-TENG achieves a maximum peak power density of 0.21 $W{\cdot}m^{-2}$ under a frequency of 2 Hz and an oscillation angle of 5°.

3.1.2. A cylindrical TENG based on a rotating-disk structure

In order to improve the output, wear resistance, and durability of TENGs, a super-durable and low-wear TENG has been designed using animal fur (Fig. 3(d)) [80]. During the rotating period, the fur

Table 1
Detailed comparison of the EMG and TENG in terms of mechanisms, advantages, and disadvantages [44,76].

Mechanical energy harvesting	Harvesting principle	Impedance type	Pros	Cons	Fundamental principles	Governing equations
EMG	Electromagnetic induction	Resistive	High efficiency and easy to scale up	Heavy magnet required and low output for small-scale devices	$\boldsymbol{E}_{\mathrm{m}} = n \cdot S \cdot w$	$\boldsymbol{E} = n \cdot \frac{\Delta\phi}{\Delta t}$
TENG	CE and electrostatic induction	Capacitive	Large output power, high effective materials, and simple fabrication	Pulsed output and high matched impedance	$\lvert I\rvert = \frac{n}{\pi} \cdot \sigma \cdot S \cdot w$	$I = n \cdot \frac{\sigma Q}{\sigma t}$

$\boldsymbol{E}$: the electric field, $\boldsymbol{E}_{\mathrm{m}}$: the peak value of $\boldsymbol{E}$, n: the number of turns of the coil, S: the coil area, w: the angular velocity, $\Delta\phi$: the amount of change in magnetic flux, I: induced current, σ: the electric charge density, Q: the charges, t: time.

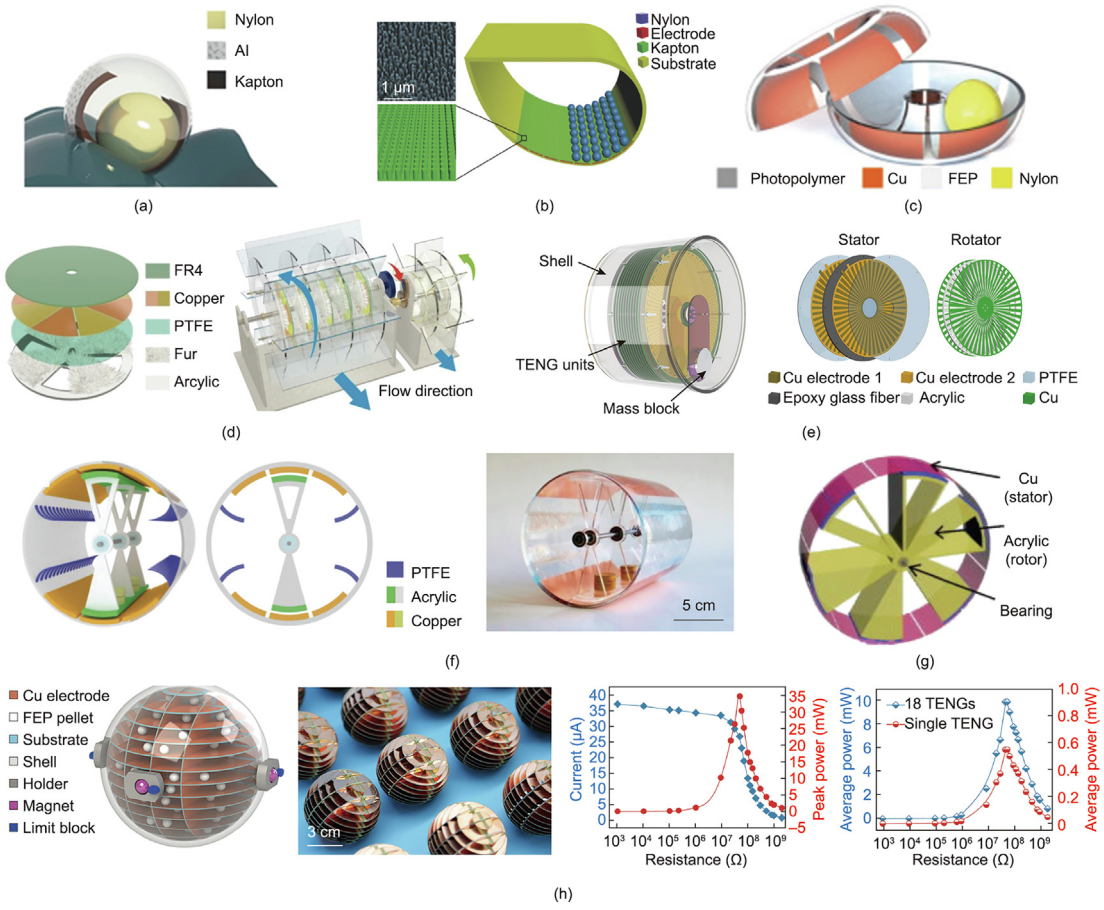

Fig. 3. Freestanding-mode TENGs for water energy harvesting. (a) Schematic configuration of the fully enclosed (RF)-TENG device operating in a water wave system; (b) schematic diagram of a freestanding duck-shaped energy harvester; (c) structure of a freestanding torus-structured (TS)-TENG based on a rolling contact mode; (d) illustrations of the material composition of the TENG, including an electrode disk and fur disk, and a waterwheel structure for water flow energy harvesting; (e) schematic illustration of the structure of the tandem disk (TD)-TENG; (f) schematic illustrations and photographs of the 3D structure and cross-section of a swing-structured (SS)-TENG device; (g) schematic diagram of a cylindrical TENG comprising an acrylic shell with Cu electrodes and a rotor adhered to fluorinated ethylene propylene (FEP) films; (h) schematic structure of a TENG unit and internal 3D electrode ball. The peak power and average power of the TENG network under water wave agitation are also shown. FR4: fiberglass cloth. (a) Reproduced from Ref. [77] with permission, (b) reproduced from Ref. [78] with permission, (c) reproduced from Ref. [79] with permission, (d) reproduced from Ref. [80] with permission, (e) reproduced from Ref. [81] with permission, (f) reproduced from Ref. [82] with permission, (g) reproduced from Ref. [83] with permission, (h) reproduced from Ref. [84] with permission.

makes tight contact and maintains low friction because of its elasticity and softness. Due to the low friction with other triboelectric materials, the fur-brush TENG achieves a high output performance and low wear. Furthermore, the performance of the fur-brush TENG is resistant to a humidity change from 40% to 90%. To further improve the output, the relative rotation speed between the rotor and stator was doubled by adding a pair of meshing gears. The fur-brush TENG can harvest wind and water flow energy, achieving a peak power density and average power density of 5.02 and 2.40 $W{\cdot}m^{-2}$, respectively. Since there is little friction and wear from the soft fur, the transferred charge of the fur-brush TENG has only 5.6% attenuation after 300 000 cycles at 0.1 N·m. Moreover, the output current of the TENG can be increased by 36.6% through the relative rotation of the fur disk and electrode disk, as realized by the counter-rotating structure.

A radial grating disk structure has been demonstrated based on an expandable tandem disk (TD)-TENG for self-powered water-quality monitoring (Fig. 3(e)) [81]. In the structure, TENG units are arranged in tandem with two hanging mass blocks on both sides. The TD-TENG employs swinging mass blocks and surface modifications to improve the average power, allowing low-frequency water wave agitation to be converted into high-frequency electrical output. The TD-TENG achieved a maximum peak power of 45.0 mW and an average power density of 7.3 $W{\cdot}m^{-3}$ in real wave tank tests. In addition, after a facile power management circuit, the TD-TENG achieved a short-circuit current of 11 mA, which is a great advance over reported currents.

3.1.3. Swing-structured (SS)-TENG

To harvest ultra-low-frequency water wave energy, a robust SS-TENG was designed by Jiang et al. [82] (Fig. 3(f)). Flexible dielectric brushes and an air gap between the triboelectric layers and electrodes contribute to the low frictional resistance. As the main part of the SS-TENG, a bearing-based swing component is supported by two circular acrylic disks. The inner wall of the SS-TENG is attached to six Cu electrodes of equal size and four groups of thin polytetrafluoroethylene (PTFE) stripes. The PTFE stripes act as a charge pump for the triboelectric charges to maintain the output. Furthermore, using anti-friction bearings or adding lubricating oils to the bearing connections significantly decreases the frictional resistance. Under external regular triggering conditions, the SS-TENG achieves a maximum peak power of 4.56 mW and an average power of 0.48 mW under the motor parameters of 7.00 cm and 7.50 $m{\cdot}s^{-2}$. The SS-TENG has excellent durability. When triggered by a single water wave, the SS-TENG achieves a maximum swing time of 88 s. Due to its low friction resistance, the SS-TENG can harvest ultra-low-frequency energy.

As shown in Fig. 3(g), a TENG based on an internal swing structure with a bearing component has been developed [83]. The cylindrical TENG consists of two main parts: a bladed acrylic rotor adhered with fluorinated ethylene propylene (FEP) film and a stator acrylic shell attached by 12 copper electrodes, each sized 25 mm × 40 mm × 30 μm. In order to improve the swing time of the rotor under an external excitation, the rotor is fabricated with a total of six hollow or solid blades, such that the barycenter of the rotor deviates from the central axis of the bearing. Due to the high utilization of the device space and the freedom of oscillation, this cylindrical TENG achieves a more stable and denser output than the pendulum-like TENG. Moreover, the cylindrical TENG has almost zero frictional resistance, because the rotor attached to FEP dielectric films can be suspended over the static metal electrodes instead of coming into direct contact with them. The cylindrical TENG can swing for 85.00 s and generate 1.39 mJ of electric energy under one excitation. It achieves a peak power density of 231.6 $mW{\cdot}m^{-3}$ and an average power density of 39.8 $mW{\cdot}m^{-3}$.

3.1.4. The 3D electrode TENG

Yang et al. [84] designed an encapsulated high-performance TENG unit consisting of 3D electrodes and self-adaptive magnetic (SAM) joints (Fig. 3(h)). In each 3D electrode, the electrode plates are encapsulated in a spherical shell. The copper layers on the electrode plates are connected to form a pair of 3D electrodes. FEP pellets are placed in the internal channels of the 3D electrode ball. The SAM joints positioned around the cell consist of a rotatable spherical magnet and a limit block. The FEP pellets roll and run through the internal channels between the two 3D electrodes under external mechanical excitations. As the pellets roll, the surface of the FEP pellets is negatively electrified, and the copper electrodes are positively electrified. The back-and-forth motion of the electrified FEP pellets converts the mechanical energy into electrical energy, generating an AC. The 3D electrode structure greatly increases the contact interface, improving the charge and power output. The 3D electrode achieves a maximum peak power density of 32.60 $W{\cdot}m^{-3}$ and a maximum average power density of 8.69 $W{\cdot}m^{-3}$ with ideal agitation in the air. A network of 18 TENG units achieves a high average power of 9.89 mW, making this an excellent method for efficiently harvesting water wave energy.

3.2. The contact-separation mode TENG for water energy harvesting

3.2.1. Spring-assisted structure

Due to the low frequency of the waves, most of the TENGs designed for harvesting water wave energy are designed to correspond to a water wave frequency of 0.03–1.00 Hz, which generates low output frequency and power. To improve the energy conversion efficiency, a spring structure has been introduced that multiplies the output frequency. When triggered by a water wave, the spring structure transforms a low-frequency motion into a higher frequency oscillation by storing the elastic potential energy from multiple cycles for later conversion into electricity afterward.

In 2017, Jiang et al. [85] presented a single-spring-assisted TENG consisting of an acrylic box and a spring connected to two Cu-PTFE-covered acrylic blocks. More specifically, two internal walls of the box-like device are anchored to the two Cu electrodes. A small circular iron is embedded into each acrylic block, increasing the contact force and contact area. As shown in Fig. 4(a) [85], a piece of an iron is sandwiched between an acrylic block bonded with Cu-PTFE film and another pristine acrylic block. The motor acceleration, spring rigidity, and spring length can greatly affect the outputs of the TENG, and the spring rigidity or spring length has been optimized to permit the spring-assisted TENG to achieve the highest output [85]. With the spring structure, the accumulated charge of the TENG is improved by 113.0%, and the translated electric energy or efficiency is increased by 150.3%.

A new spherical TENG that couples a spring-assisted structure with a swing structure was designed and encapsulated in an outer acrylic spherical shell that floats on the ocean surface (Fig. 4(b)) [86]. In the acrylic spherical shell, two bearings are fixed to the inner wall, and an axis is integrated with a swing component. To lower the center of gravity, a copper mass ball is embedded at the bottom of the swing part. Adhered to the spherical shell, two middle acrylic sheets and springs support four movable acrylic sheets. Under water waves, the swing component swings left and right. This TENG achieves an output current of 56.2 μA and an output power of 4.1 mW under real water waves of 1 Hz and 10 cm. The spring raises the frequency to enhance the output. The swing part impacts the spring component, decreasing the swing period and increasing the frequency. Moreover, the spring structure increases the contact force between the triboelectric materials of the TENG unit and enhances the reciprocation of the swing part.

These spring TENGs are designed to be in a vertical or axial spring vibrational mode in order to harvest vibrating energy in that direction. However, the springs are not used in the TENG to harvest horizontally oriented vibration energy. A helical structure TENG integrated with a spring was developed to integrate a TENG with a spring for arbitrary-direction vibration energy harvesting (Fig. 4(c)) [87]. This helical TENG is composed of two conductive elastomeric layers and two nonconductive elastomeric layers. Due to the assistance of soft silicone rubber and a wire spring, both vertical and horizontal vibration excitations change the distance between the helical structure's adjacent coils. The TENG can also be used as a self-powered active sensor to sense the acceleration and frequency of vibration. It achieves a maximum average power density of 45.0 $mW{\cdot}m^{-2}$ under a vertical resonance vibration of 16.0 Hz and a horizontal resonance vibration of 8.5 Hz.

3.2.2. Mass-spring structure

The mass-spring structure can be tuned to match the frequency of the external agitations in order to achieve resonance, which can generate electricity when triggered by water waves. A self-powered intelligent buoy system (SIBS) with a multilayered mass TENG was developed for harvesting water wave energy by Xi et al. [88] in 2019. As shown in Fig. 4(d), the multilayered TENG consists of six basic units, in which two round FEP films are attached on both sides of the mass, and sponges serve as a buffer [88]. On both sides of the mass, two springs with an elastic coefficient of 50 $N{\cdot}m^{-1}$ and a length of 40 mm are fixed. Under water waves, the mass vibrates from the top and bottom Cu films in cycles, generating AC electricity. This multilayered TENG can produce an open-circuit voltage of 250 V and a short-circuit transferred charge of 3 μC. The output voltage of the multilayered TENG can be converted and regulated as a steady direct current (DC) voltage of 2.5 V by means of a power management module (PMM). The multilayered TENG achieves an average output power density of 13.2 $mW{\cdot}m^{-2}$. This TENG was used in the first demonstration of a complete TENG-based micro-energy strategy for a self-powered intelligent system, including energy harvesting, management, deployment, and utilization.

3.2.3. Multilayered structure

A multilayered structure can enlarge the contact area of a TENG, which is an effective method for greatly improving the output. A spherical TENG with a spring-assisted multilayered structure for harvesting water wave energy was developed by Xiao et al. [89] in 2018 (Fig. 4(e)). This TENG possesses the advantages of a spring structure and an integrated multilayered structure. An aluminum electrode and a polarized FEP film come into contact and separate to generate electricity. Inside the shell, four steel shafts are fixed

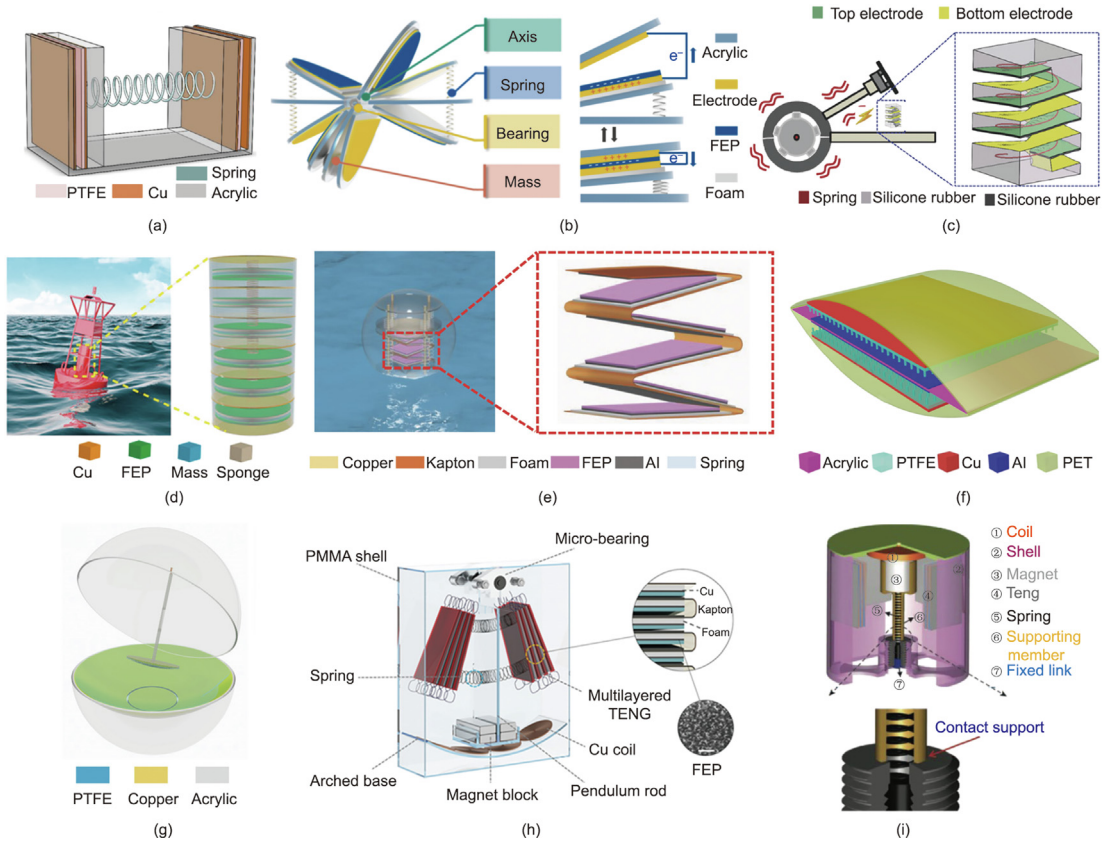

Fig. 4. A contact-separation-mode TENG structure for water energy harvesting. (a) Schematic structure of the spring-assisted TENG structure; (b) schematic diagram for the enlarged structure inside the spring-assisted swing TENG; (c) schematic diagram of a helical TENG; (d) structural diagram of a designed multilayered TENG in a buoy; (e) schematic illustration of a spherical TENG with a spring-assisted multilayered structure floating on water; (f) schematic structure of an as-fabricated minimum functional unit; (g) schematic structure of a TENG composed of a cambered triboelectric layer and a pendulum-like component; (h) structure and materials design of the device; (i) schematic diagram of a hybridized TENG. (a) Reproduced from Ref. [85] with permission, (b) reproduced from Ref. [86] with permission, (c) reproduced from Ref. [87] with permission; (d) reproduced from Ref. [88] with permission, (e) reproduced from Ref. [89] with permission, (f) reproduced from Ref. [90] with permission, (g) reproduced from Ref. [91] with permission, (h) reproduced from Ref. [92] with permission, (i) reproduced from Ref. [93] with permission.

between circular acrylic blocks adhered to the internal wall of the sphere. To protect the mass block from a collision with the top acrylic block, four rigid springs are attached to the top side of the mass part. To ensure sufficient contact, two 4 mm thick acrylic blocks are attached on the bottom side of the multilayered TENG. A zigzag structure is fabricated using a 12.5 μm thick FEP film as the dielectric layer and two pieces of aluminum foil as the electrodes. The TENG array generates an output current of 225.00 μA and a maximum output power of 15.97 mW under water waves.

A TENG network with arch-shaped top and bottom plates and a multilayered core has been developed (Fig. 4(f)) [90]. After heat treatment, polyethylene terephthalate is bent to form the top and bottom plates. Due to the elasticity of the film, the TENG generates electricity. The material core of the upper and bottom layers is PTFE film, upon which copper deposits to form back electrodes. In order to improve the triboelectric charge density, the PTFE surface is modified by PTFE nanowire arrays through reactive ion etching. Thanks to its good strength, light weight, good machinability, and low cost, acrylic was selected as the structural supporting material. The TENG is expected to generate an average power output of 1.15 MW over a water area of 1.00 km^2.

3.2.4. Pendulum-like structure

With swinging mass blocks, a TENG with a pendulum-like structure can transform and store potential energy in order to output electricity. Under mechanical excitation, the pendulum-like structure converts the impact agitations into continuous swinging for an extended period of time. An elastic-connection and soft-contact TENG with a pendulum-like structure has been developed, exhibiting simultaneously boosted durability and efficiency (Fig. 4(g)) [91]. This pendulum-like TENG is sensitive to external mechanical excitation with an air gap between the triboelectric layers. The TENG works in a non-contact mode, which enhances its robustness and durability. In addition, the pendulum's spring and flexible dielectric fluff achieve an elastic connection and soft contact. The surface triboelectric charges of the TENG can be replenished by mechanical excitation for high efficiency with multiplied frequency. The TENG achieves a maximum peak power of 28.0 μW, a high energy conversion efficiency of 29.7%, and excellent durability after continuous operation for two million cycles.

Based on an optimized pendulum structure, a hybrid nanogenerator with a TENG and an EMG with four Cu coils was developed by Ren et al. [92] in 2021 (Fig. 4(h)). This TENG can send high-frequency warning information to a terminal on a boat, providing valuable information for boat safety under severe sea conditions such as unforeseen fog or rainstorms. The triboelectric part of the nanogenerator consists of six pairs of contact-separation-mode, which use polyimide film (Kapton) as the backbone. FEP and Cu films are attached to the Kapton film. The EMG part consists of a wobbly magnet block and four Cu coils, utilizing the space within the device. The magnet block acts as a mass block to provide motion inertia for the pendulum. Optimized springs are attached on two sides of the pendulum rod to tighten the contact of the triboelectric layers and to avoid an excessive swing amplitude of the

pendulum. The single TENG achieves an output power of 1.72 mW and a power density of 0.41 $W \cdot m^{-2}$.

A non-resonant hybridized electromagnetic-TENG was developed by Xie et al. [93] for obtaining all-dimensional vibration energy (Fig. 4(i)). The nanogenerator has eight main parts: four TENGs, a magnet support, a coil, a cylindrical NdFeB magnet, a spring, an end cover, a hollow cylindrical shell, an adjusting stud, and a locking screw. The oscillating part of the TENG is supported on a fixed surface by a spring and is swung as a sphere around the support. Because of its elasticity, the TENG can reduce the energy loss caused by the collision between the magnet and the outer wall. The TENG achieves a total power of 470.0 μW under a loading resistance of 0.5 MΩ, and the EMG provides 523.0 mW at most under a loading resistance of 280.0 Ω. The energy conversion efficiency of the hybridized system is 48.48%.

4. Performance enhancement strategies for TENGs in blue energy harvesting

Developing TENGs as a new type of power generation technology to collect blue energy has become a major research topic in the field of clean and renewable energy. However, there is still a long way to go before commercialization can be realized. The main problem is that it is difficult for the performance of TENGs under water waves to meet commercial standards. In recent years, researchers have explored a series of performance enhancement strategies for TENGs designed for blue energy harvesting from different perspectives.

4.1. Materials and structural optimization

The efficiency of blue energy harvesting mainly depends on the TENG output under water waves. Above all, material optimization is the basis of TENG performance enhancement [63,88]. An effective solution is to select materials with a large difference in their electronegativities, according to the triboelectric series [64,89,94,95]. In 2021, Feng et al. [83] were the first to introduce soft and dense rabbit fur into a SS-TENG device for harvesting blue energy. Compared with most triboelectric materials, rabbit fur has been found to be strongly electropositive. In the device, the rabbit fur provides charge replenishment, improving the charge density on the triboelectric surface and the output performance of the TENG. The rabbit fur can also reduce the frictional resistance and material wear. In subsequent works, rabbit fur has become a common material choice.

In addition to choosing reasonable materials, researchers have modified the surfaces of materials used for TENG fabrication by means of micromachining or chemical methods to construct micro-nano structures. Chen et al. [90] created nanowire arrays on a PTFE surface via a top-down method through reactive ion etching, which largely enhances the charge density in CE. Surface functionalization can affect the electrification properties of materials, thereby improving the output performance of TENGs. Designing a soft contact mode is another promising direction for material optimization. Cheng et al. [35] fabricated a rolling flexible liquid/silicone ball as the soft core to construct a soft-contact spherical TENG (SS-TENG), which significantly increases the contact area. The SS-TENG exhibits a 10-fold enhancement in maximum output charge compared with a conventional ball-shell TENG based on the hard-contact mode. It is also feasible to start with an electrode material to construct a TENG in soft-contact mode. Xiao et al. [89] fabricated a TENG with a silicone rubber/carbon black composite electrode. The silicone-based electrode with soft texture provides an improved contact effect when used with dielectric film as the other surface.

Moreover, a reasonable structural design can optimize the interaction between a TENG device and water waves, enhancing the working effect of the TENG. In Section 3, various TENG structures were systematically classified and summarized, including the original ball-shell structures, 3D electrode structures, effective spring structures, durable pendulum structures, and others. Through the continuous optimization of these structures, the output performance and the water wave energy conversion efficiency of the TENG devices are gradually improved.

In summary, materials and structural optimization are the most direct methods to enhance the performance of TENGs used for blue energy harvesting and hold great significance for the commercialization of these TENGs.

4.2. Hybrid energy harvesting

Compared with traditional energy harvesting methods, TENGs have some unique characteristics, including a high voltage, low current, and high energy conversion efficiency. Integrating other energy harvesting methods with TENGs to combine their respective advantages is considered to be an effective performance enhancement strategy.

In recent years, many scholars have conducted systematic research on hybrid nanogenerators with TENGs and EMGs. In 2019, Hou et al. [96] proposed a rotational pendulum triboelectric–electromagnetic hybrid generator for water wave energy harvesting. The structure of the device, as shown in Fig. 5(a) [96], includes a pendulum rotor (magnets and a Cu ring), coils, TENG blades, and a cylindrical frame. The magnets and coils form an EMG module, while the blades and Cu ring form a contact–separation TENG module. The researchers placed the device in a laboratory-simulated water wave environment, verifying the device's feasibility for collecting water wave energy. A simple buoy based on this device was also fabricated and applied in Taihu Lake. In the same year, Chen et al. [97] reported a chaotic pendulum triboelectric–electromagnetic nanogenerator for wave energy scavenging; a structural diagram is shown in Fig. 5(b). This device consists of TENG units in freestanding mode and EMG units. The TENG units are fixed onto the sector of the central pendulum, while the EMG units are set inside the sandwiched space of the central pendulum. Unlike the two pendulum structures described above, Wu et al. [34] designed a spherical hybrid nanogenerator by dividing multilayered spaces, as shown in Fig. 5(c). The magnetic sphere in the device not only serves as an element of the EMG but also drives the TENG below. Similarly, the device shown in Fig. 5(d) [98] is divided into multiple parts. In the device, each chamber is equipped with a TENG unit, and the two outermost chambers are equipped with EMG units.

Aside from EMGs, combining piezoelectric nanogenerators (PENGs) with TENGs to fabricate hybrid energy collectors is an effective direction for blue energy harvesting in some cases. Fig. 5(e) shows a triboelectric–electromagnetic–piezoelectric hybrid nanogenerator proposed by Tian et al. [99] in 2022. The device is a semi-cylindrical structure that contains one TENG unit, two EMG units, and two PENG units. The shell and slider together form the TENG unit, while the coils and magnets on the cantilever beam form the EMG unit and the PENG units are attached to the root of the cantilever beam. Due to the repulsion between the magnets, the cantilever beam can vibrate at a high frequency, driving the PENG units to generate electric charge. The introduction of PENGs further enriches the working modes of the hybrid generator and improves the output performance.

Oceans contain multiple energy sources, of which ocean wave energy is just one example. Developing hybrid generators that can collect wave energy and other forms of energy at the same time could improve the efficiency of ocean energy harvesting.

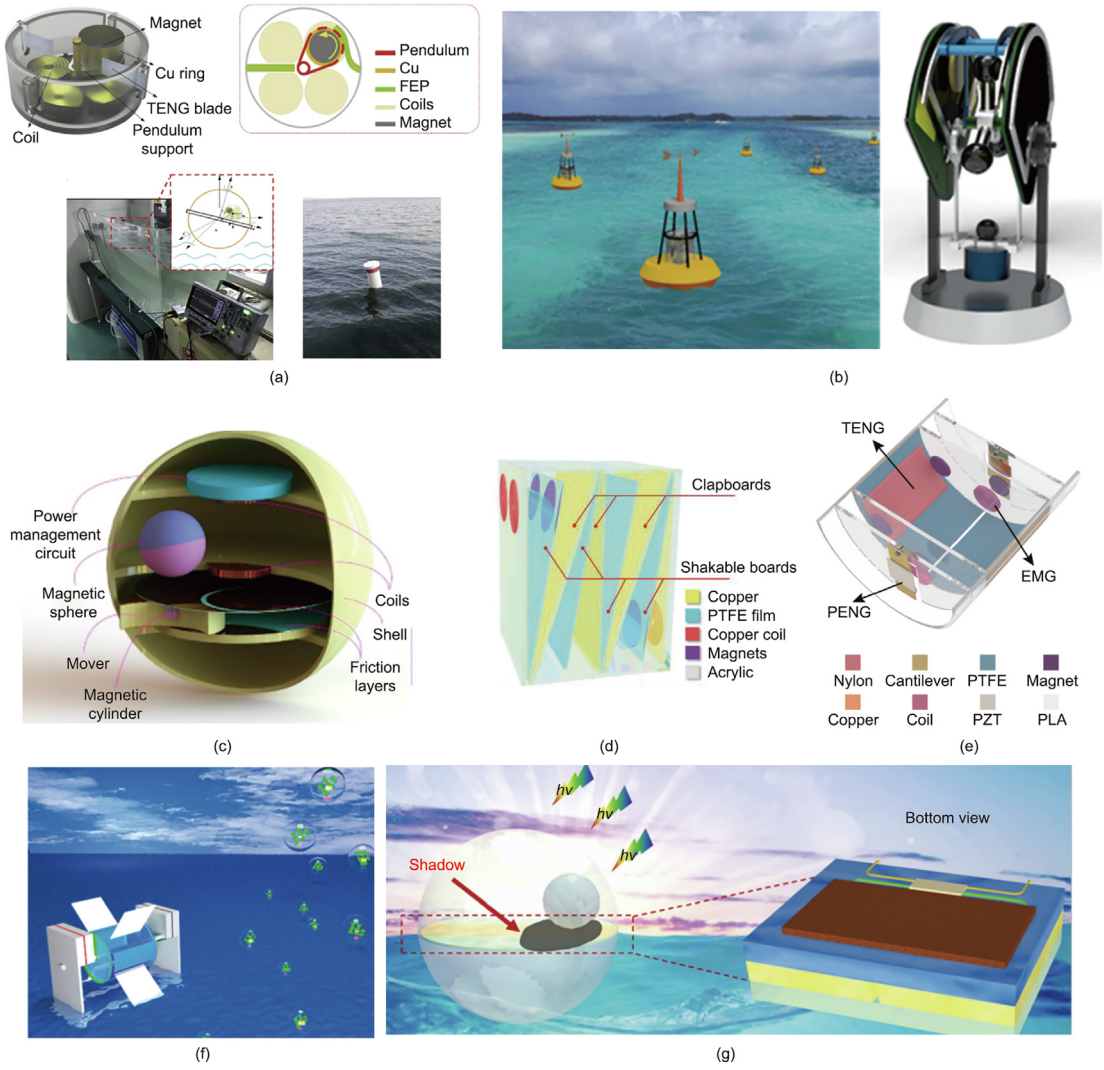

Fig. 5. (a) Rotational pendulum triboelectric–electromagnetic hybrid generator; (b) chaotic pendulum triboelectric–electromagnetic nanogenerator for wave energy scavenging; (c) spherical triboelectric–electromagnetic water wave energy harvester; (d) hybrid harvester designed based on a pivot hinge; (e) triboelectric–electromagnetic-piezoelectric hybrid nanogenerator; (f) schematic diagram of a TENG device utilized to simultaneously harvest wind energy and water wave energy; (g) shadow–tribo-effect nanogenerator with a hybrid tribo-effect and shadow-effect. PZT: lead zirconate titanate piezoelectric ceramics; PLA: polylactic acid. (a) Reproduced from Ref. [96] with permission, (b) reproduced from Ref. [97] with permission, (c) reproduced from Ref. [34] with permission, (d) reproduced from Ref. [98] with permission, (e) reproduced from Ref. [99] with permission, (f) reproduced from Ref. [100] with permission, (g) reproduced from Ref. [101] with permission.

Fig. 5(f) exhibits a TENG device that simultaneously harvests wind and wave energy, which was reported by Zhu et al. [100] in 2021. The combination of solar energy with wave energy is another good direction. Zhang et al. [101] proposed a shadow–tribo-effect nanogenerator that combines a tribo-effect and a shadow effect, as shown in Fig. 5(g). This spherical device can float on the ocean surface and be illuminated by the sun. Under dark conditions, the working mechanism of the device is mainly based on the tribo-effect, and the output power is in the form of AC pulses. Under light illumination, the shadow effect is dominant, and the device produces DC output. In this work, the researchers utilized two energy harvesting methods to realize efficient ocean energy harvesting.

4.3. Network designs

Compared with the vast ocean surface, the size of a single TENG unit is tiny, so the scale of water wave energy harvesting is limited. In 2014, Wang [38,102] proposed the idea of connecting multiple TENG units into networks to harvest ocean wave energy, which is an excellent way to increase the scale and output performance. Recently, researchers have developed various proposals for TENG networks.

The simplest way to integrate TENG units is by building one-dimensional (1D) chain structures. In 2019, Xu et al. [103] conceived a chain structure extending upwards from the ocean floor (Fig. 6(a)) based on a tower-like TENG unit. This scheme utilizes the energy in the deep sea, and avoids occupying the sea surface, thereby reducing adverse impacts on human life. The 1D chain structure can also be arranged along the direction of ocean waves. Figs. 6(b) and (c) [81,104] provides two typical examples. The device shown in Fig. 6(b) was derived from the Pelamis Snake energy harvester [104]. As a wave passes through, the chain can flex and bend easily to output electrical energy. The structure in Fig. 6(c) is based on a TD-TENG unit [81], with a rope from the bottom linking the units. Placing the units in reasonable connection positions can optimize the movement of each TENG unit in the chain structure, enhancing the output performance.

Another common integration method involves developing two-dimensional (2D) planar structure networks for water wave energy harvesting on the sea surface. Fig. 6(d) provides a schematic diagram of a large-scale network designed by Chen et al. [90] in

2015. This TENG network has a square shape, and a multi-level structure is introduced in the scheme. The entire TENG network consists of multiple modules, where each module is composed of a certain number of TENG units. This is a very simple and efficient integration scheme, and many later TENG network designs draw on this work. For example, Fig. 6(e) exhibits a photograph of a 4×4 TENG network fabricated by Xu et al. [72] in 2018. Apart from the square structure, researchers have tried to explore other integration methods to construct TENG networks in different shapes. In 2019, Liang et al. [51] reported a hexagonal TENG network, as shown in Fig. 6(f). This network consists of seven spherical spring-assisted TENG units, which are respectively distributed at the six vertices and center of the hexagon.

In addition to the shape of the TENG network, the connection mode between units in the network affects the overall performance in a water wave environment. In 2019, Yang et al. [84] proposed a self-assembling TENG network whose unit is based on a 3D electrode structure. By attaching rational SAM joints on the spherical shell of each TENG unit, the researchers successfully achieved self-assembly, self-adaptation, and self-healing of the TENG network, as shown in Fig. 6(g) [84]. This scheme improves the efficiency of TENG networking and maintenance, making it of great significance to blue energy commercialization. However, at present, there is scant related research work and the scheme is still in a preliminary stage, with further exploration required.

4.4. Power management

Driven by mechanical force, TENG devices directly generate electrical energy in the form of AC pulses. It is difficult for back-end functional circuits to effectively use this kind of electrical energy, limiting the practical applications of TENGs. To solve this problem, researchers have developed effective power management schemes. A combination of power management schemes is obviously necessary for blue energy harvesting, because the output of TENGs under water waves is irregular. Power management is regarded as an important performance enhancement strategy for blue energy exploitation.

The framework of a power management system for water wave energy harvesting is illustrated in Fig. 7(a) [51]. First, the TENG network harvests water wave energy and produces AC output. Next, the PMM converts the signals into DC output. Finally, the DC output is utilized to power general functional circuits, including sensors, displays, and wireless transmitters.

At present, the most commonly used PMM is based on DC buck conversion, which was first reported by Xi et al. [48] in 2017. In 2019, Liang et al. [51] applied this module to water wave energy harvesting; a detailed circuit diagram is depicted in Fig. 7(b). The module contains an autonomous switch, an inductor, a capacitor, and some diodes. It can extract the maximum electrical energy generated by the TENG network by means of the autonomous switch. The inductor and capacitor act as a low-pass filter to convert the irregular voltage into a stable DC voltage. The output performance of the TENG network connected to the module is shown in Fig. 7(c) [51]. It can be seen that the output voltage curves are stable DC signals, regardless of the load resistance. The introduction of this module can significantly increase the charging speed of a TENG network. Fig. 7(d) [51] reveals a comparison of the charging speed of a TENG network with or without the module, showing that the charging speed increased by 96 times for a 10 mF capacitor with the module. Based on this module, Xi et al. [88] exploited a SIBS for water wave energy harvesting. A circuit diagram of the system is shown in Fig. 7(e) [88]. A regulator and stabilizer further improve the utility of the module. Fig. 7(f) shows the output voltage curves of a power-managed TENG with different load resistances [88]. The voltage curves are all stable at 2.5 V, while the duration periods are different according to the energy consumption on the load. The researchers also measured the relationship of voltage U and transferred charge Q (U–Q curve) and compared it with the theoretical maximum, as shown in Fig. 7(g) [88]. The result indicates that 70.3% of the energy is autonomously transferred to the module from the TENG, demonstrating the high working efficiency of the module.

4.5. Charge excitation

In recent years, researchers have developed effective charging-pump and charge-excitation schemes to improve the output performance of general TENGs [105–108]. These methods are simpler and more effective than material optimization and structural design. It is clear that a combination of these methods is a promising way to realize TENG performance enhancement for blue energy harvesting.

In 2020, Wang et al. [109] demonstrated a high-performance TENG for water wave energy harvesting based on charge shuttling. The structure and circuit connection of the TENG device are shown in Fig. 8(a) [109]. The TENG device is divided into two parts: the left phase and the right phase. The charges generated by the left-pump TENG are accumulated in the main TENGs (M-TENGs) L1 and L2 through the rectifier bridges, and the right phase is similar. Through charge accumulation, the output performance of the entire TENG device is greatly enhanced. Fig. 8(b) [109] shows the output power of the TENG, indicating that the maximum output power reaches 126.67 mW and the power density is 30.24 $W \cdot m^{-3}$, which is a huge improvement over ordinary TENGs.

Charging-pump and charge-excitation schemes have been applied to TENG network development, in addition to adding them to individual TENG units. Fig. 8(c) shows a schematic diagram of a self-charge-supplement (CS)-TENG network, which was designed by Jiang et al. [110]. This network contains one CS-TENG and several M-TENGs. The CS-TENG is an ordinary TENG using the contact–separation mode, while the M-TENGs are composed of three layers. The CS-TENG serves as a charging pump, and the charges generated are accumulated in the M-TENGs, which is an effective solution to prevent charge dissipation. When the TENG network operates in water waves, the potential difference between the electrodes of the M-TENGs drives the current flow through the external load, generating a periodic AC. The researchers explored two different connection modes of the network, for which the connection positions of the CS-TENG and M-TENGs are different. Figs. 8(d) and (e) shows the transferred charge and output voltage of the network with or without the charge-supplement scheme. Regardless of the connection mode, the output performance of the charge-supplement network is significantly superior to the direct output [110]. The research group also proposed a charge-excitation TENG network in 2020 [111]. In this work, a charge excitation circuit (CEC) based on series-parallel switching is specially designed for a TENG intended for water wave energy harvesting. When integrated with the CEC, the TENG's output current improved, and the AC output was converted to DC output. Therefore, charge excitation TENG units can be directly connected to a network without rectifier bridges. A circuit diagram is shown in Fig. 8(f) [111]. In order to verify the working effect of the CEC, the researcher systematically measured the output performance of the TENG network under different water wave conditions. Fig. 8(g) shows the output current of the TENG network with CECs. The maximum value reached 24.5 mA at a water frequency of 0.6 Hz, which is much higher than that of ordinary TENG networks [111]. The output power reached 24.60 mW, and the peak power density was calculated as 6.71 $W \cdot m^{-3}$ (Fig. 8(h)) [111]. These results illustrate that the combination of charge-pump and charge-excitation schemes

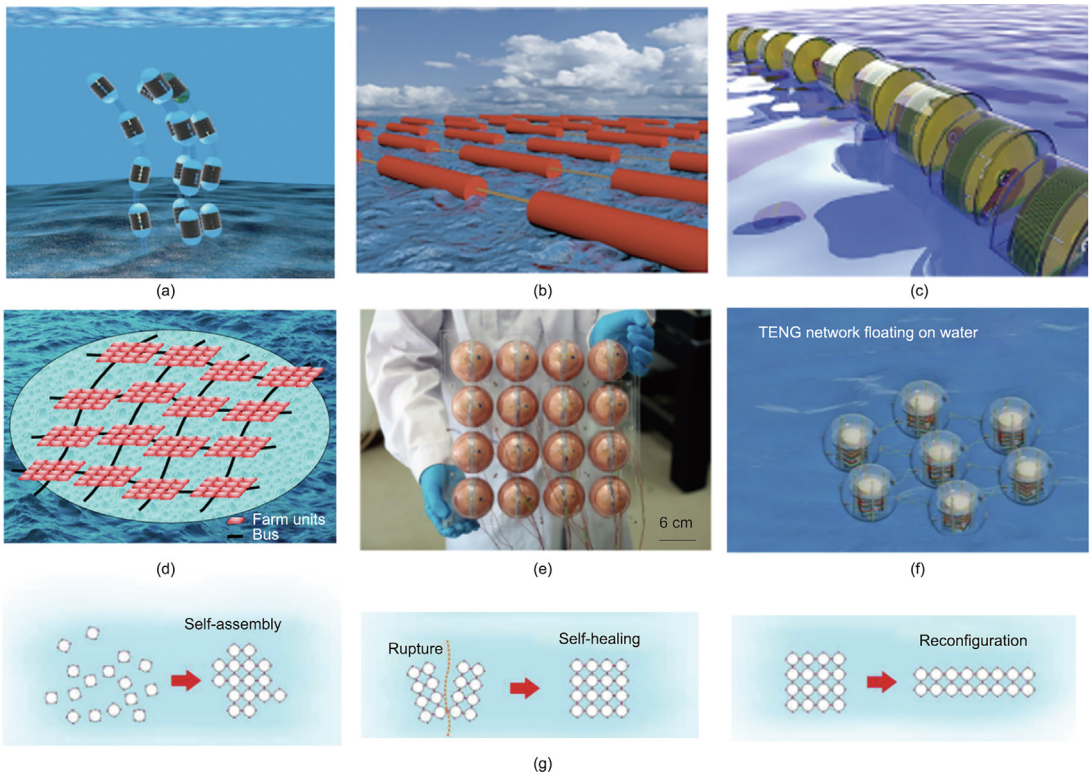

Fig. 6. (a) TENG network with a chain structure extending upwards from the ocean floor; (b) sea snake composed of TENG units; (c) TENG network based on a TD-TENG device; (d) configuration of a quadrilateral network with multilayered connection; (e) photograph of square 4 × 4 networks based on a ball-shell TENG unit. (f) Hexagonal network containing seven TENG units. (g) Self-assembling TENG network with rational SAM joints. (a) Reproduced from Ref. [103] with permission, (b) reproduced from Ref. [104] with permission, (c) reproduced from Ref. [81] with permission, (d) reproduced from Ref. [90] with permission, (e) reproduced from Ref. [72] with permission, (f) reproduced from Ref. [51] with permission, (g) reproduced from Ref. [84] with permission.

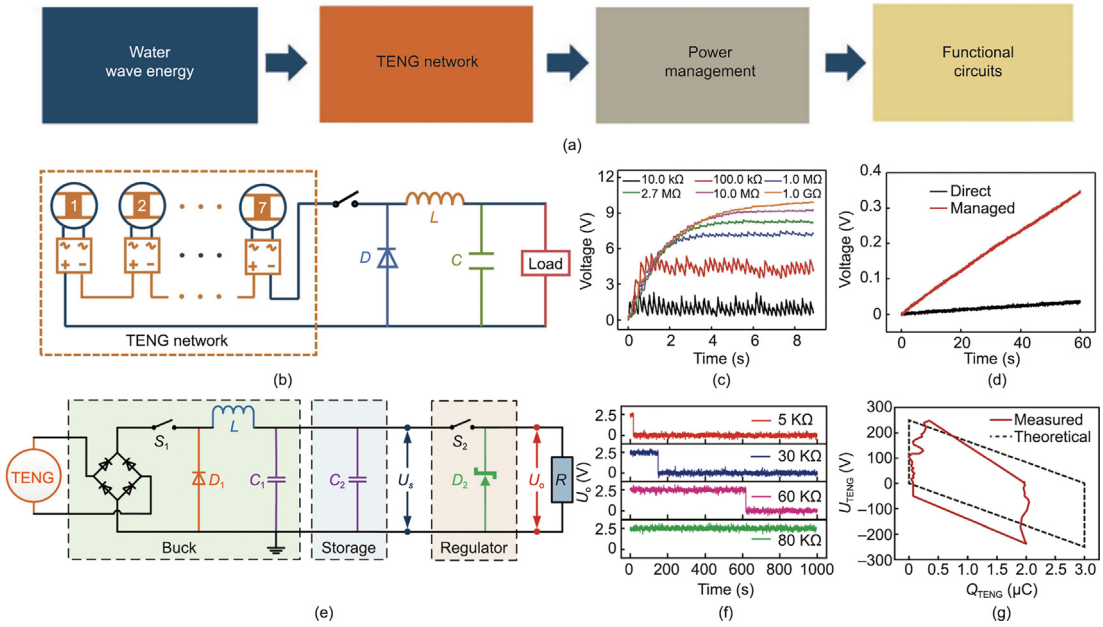

Fig. 7. (a) Framework for an integrated self-powered system driven by water wave motions; (b) schematic diagram of the power management mechanism for a TENG network; (c) output voltage on a load resistor for the TENG network, with a PMM at various resistances under water waves; (d) comparison of the charging profiles of the TENG network, between managed charging and direct charging for a 10 mF capacitor; (e) schematic circuit diagram of a SIBS; (f) output voltage of the TENG at different load resistances; (g) the voltage U and transferred charge Q (U–Q) curve of a theoretical TENG and power-managed TENG. D1 and D2: diode; L: inductor; C1 and C2: capacitor; S1 and S2: switch; R: resistance; Uo: the output voltage; UTENG–QTENG: the U–Q curve of the TENG. (a–d) Reproduced from Ref. [107] with permission, (e–g) reproduced from Ref. [88] with permission.

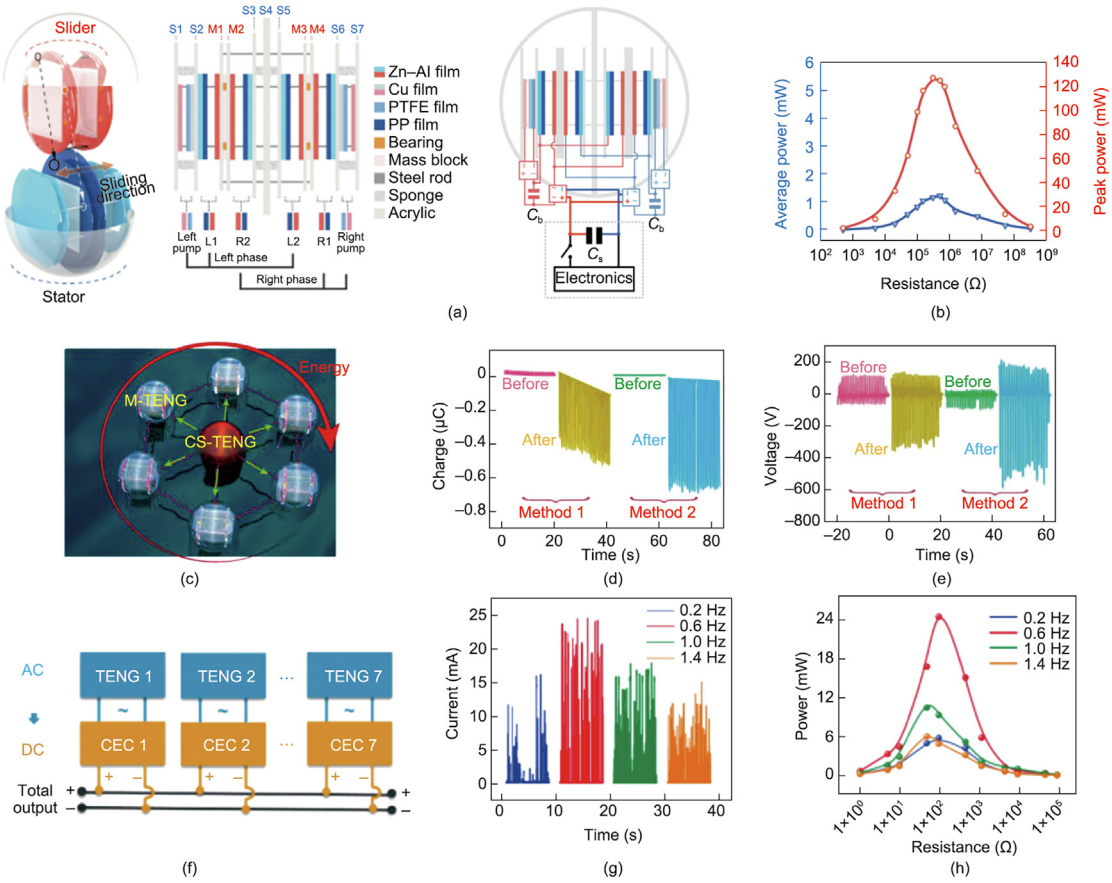

Fig. 8. (a) Structure and circuit connection of a TENG device based on charge-shuttling; (b) peak power and average power of the integrated device with various loads in water waves; (c) self-charge-supplement (CS)-TENG network; (d) transferred charge and (e) output voltage for the TENG before and after a charge supplement via two methods; (f) parallel connection of the units in the TENG network through charge excitation circuits (CECs) without rectified bridges; (g) output current and (h) output power-resistance profiles of the charge-excitation TENG network for various water waves. M-TENG: main TENG; PP: polypropylene. (a,b) Reproduced from Ref. [109] with permission, (c–e) reproduced from Ref. [110] with permission, (f–h) reproduced from Ref. [111] with permission.

with TENGs for blue energy harvesting is an effective performance enhancement strategy.

5. Marine environmental applications of TENGs based on blue energy harvesting

It is well known that environmental pollution of the ocean and natural disasters gradually negatively affect the utilization of ocean energy. Thus, ocean monitoring and sensing play a key role in developing smart oceans.

5.1. Power supply for distributed sensors and signal transmission systems in the ocean

5.1.1. Water temperature, atmospheric pressure, and humidity monitoring

Marine environment sensing technology is the basic technology of marine environment monitoring, which can convert the perceived characteristics of marine meteorology, hydrology, ecology, and other elements into appropriate electrical signals. In marine environment monitoring, various kinds of sensors are needed to monitor different physical and chemical parameters, such as water temperature, atmospheric pressure, wind speed, wind direction, pH, conductivity, humidity, and so forth.

Many TENGs have been designed to harvest water wave energy and to power distributed sensors that can monitor water temperature, atmospheric pressure, and humidity. For example, a TS-TENG consisting of an inner ball and a torus shell was developed by Liu et al. [79] in 2019 (Fig. 9(a)). The TENG harvests water wave energy and stores energy to power environmental sensors; its array charges a capacitor of 47 μF and then powers a thermometer. The thermometer is connected by a switch and functions to measure water temperature.

An ocean wave energy harvesting system driven by atmospheric pressure difference was developed by Cheng et al. [112] in 2018 (Fig. 9(b)). This TENG utilizes intermittent and low-frequency near-shore water wave movement to harvest and store energy, transforming it into airflow and later triggering continuous and high-frequency movement. Two specific TENG structures have been demonstrated: a TENG triggered by a lower speed of airflow and another TENG driven by a stronger airflow. The short-circuit current increases from 4 to 8 μA as the speed of the airflow increases from 7 to 10 $m \cdot s^{-1}$; it then decreases as the speed increases further. The short-circuit current is 6 μA when the airflow speed reaches 14 $m \cdot s^{-1}$.

In addition, a floating buoy TENG comprising an acryl-packed power generation unit, a height-adjustable support, and a floating buoy was developed by Kim et al. [113] in 2018 (Fig. 9(c)). This TENG powers a thermo-hygrometer with a 470 μF capacitor. As the TENG charges the capacitor to 2.0 V, the thermo-hygrometer

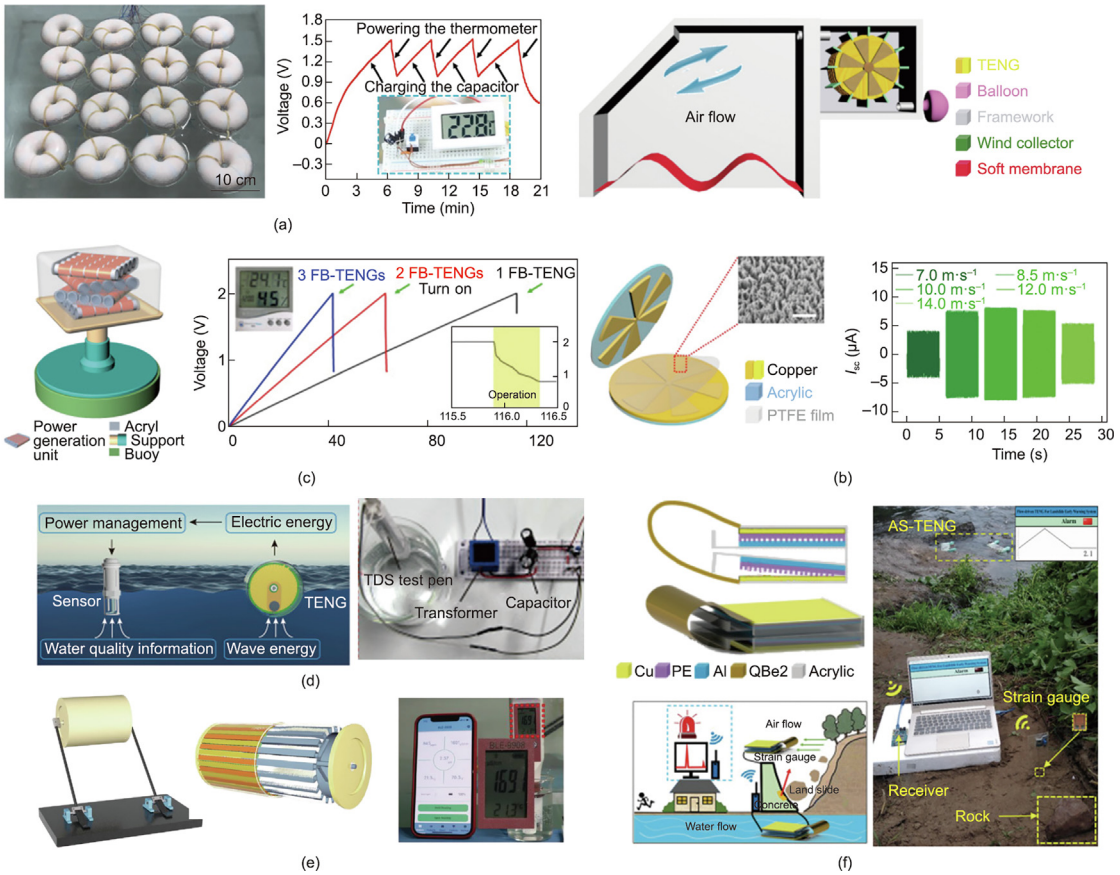

Fig. 9. (a) Photos and charge–discharge curve for a TENG array to power a thermometer; (b) schematic illustration of a TENG driven by atmospheric pressure difference; (c) schematic illustration of a floating buoy-based TENG and the charge and discharge curves of capacitors powering the thermo-hygrometer; (d) schematic illustration of a self-powered water-quality monitoring system, with the side and front views of the structure of the TD-TENG; (e) structural design of a TENG, with a photograph showing it powering a wireless multifunctional pen for water-quality detection; (f) schematic diagrams of the functional components of a TENG and its powering of a wireless landslide early warning system, with a photo of the system in the natural environment. Isc: short-circuit current; TDS: total dissolved solids; AS-TENG: arc-shaped TENG; PE: polyethylene; QBe2: beryllium bronze alloy material. (a) Reproduced from Ref. [79] with permission, (b) reproduced from Ref. [112]with permission, (c) reproduced from Ref. [113] with permission, (d) reproduced from Ref. [81] with permission, (e) reproduced from Ref. [114] with permission, (f) reproduced from Ref. [115] with permission.

is turned on and the voltage drops to 1.6 V. The TENG's self-powered temperature and humidity system can provide useful information on the weather, such as the temperature and humidity at sea.

5.1.2. Water quality monitoring

Water pollution from sources including fertilizers, pesticides, sewage, oils, heavy metals, trace elements, plastics, and eutrophication presents a severe environmental issue. In order to sustainably and autonomously monitor water quality, it is necessary to develop *in situ* self-powered water-quality monitoring systems that can harvest local wave energy. Various TENG structures have been developed for self-powered water-quality monitoring.

In 2019, Bai et al. [81] developed an expandable TD-TENG on a radial grating disk structure for self-powered water-quality monitoring (Fig. 9(d)). With power management, the total dissolved solids (TDSs) test pen is connected to the TENG, whose capacitor is 14.7 mF. As the capacitor is charged to 3.5 V, the test pen is turned on by closing the switch and measures the TDS of the water. In testing, the normal operating voltage of the TDS test pen was found to be 3 V, exhibiting a much larger energy consumption than a thermometer or wireless transmitter; thus, it requires a higher power TENG.

Another TENG for water-quality monitoring uses a cylindrical wave-driven linkage mechanism, which converts the water wave motion into circular movement of the rotor and transforms the rotational energy into electricity (Fig. 9(e)) [114]. The TENG is fixed on the water's surface, and the rotor twirls under the water waves. The TENG charges a 10 mF capacitor to power a detection pen with Bluetooth transmission capability. Various data, including the water temperature, pH, TDS, and electric conductivity, are wirelessly transmitted by Bluetooth to a mobile phone.

A new recycling method that reuses waste milk cartons to fabricate TENGs has been proposed [115]. This TENG generates an open-circuit voltage of 600 V and a short-circuit current of 40 μA. Moreover, the TENG can power wireless sensor nodes for pH monitoring. As shown in Fig. 9(f), this TENG has been put in a river to power a wireless strain-gauge sensor on an acrylic board, where the resistance changes according to the acrylic board deformation [115]. When rocks tumble and hit the acrylic board, a sensing signal is sent to a remote receiver and displayed on a computer, generating a landslide monitoring alarm.

5.1.3. Wireless SOS alarm system

When a ship is in distress at sea, sending a distress signal to nearby ships or shore stations through the equipment on board helps ensure the safety of maritime traffic. However, there is currently a lack of suitable low-power sensors for information transmission. A hybrid triboelectric–electromagnetic nanogenerator based on a magnetic sphere was developed by Wu et al. [34] in 2019, which harvests the water wave energy from any orientation. This hybrid generator can harvest energy to power wireless sensor networks for environmental monitoring, including temperature, pH, and oxygen level. As shown in Fig. 10(a) [34], the hybrid device

harvests water wave energy to drive a wireless water temperature alarm system with a temperature switch. In the system, a charging voltage of over 2.75 V on the low-dropout regulator unit provides sufficient energy to power the follow-up circuit when the temperature switch is closed. The work voltage of the microcontroller unit and the wireless receiver is 3.3 V. The temperature alarm system is shown in Fig. 10(a).

A super-durable and low-wear TENG has been developed to power electrical devices in agricultural production (Fig. 10(b)) [80]. This TENG can harvest water flow and wind energy to power many sensors to monitor the environment in real time and manage fully automated agriculture. The TENG unit, which uses a free-standing mode, consists of a fur disk and an electrode disk attached to PTFE film. The TENG powers a soil moisture sensor with a 470 μF capacitor, where the sensor continuously monitors the soil moisture in real time. The TENG also harvests wind energy to power a raindrop sensor for monitoring the weather and sends an alarm when it rains.

A buoy-like liquid–solid-contact TENG, possessing four key advantages, has been developed for harnessing blue energy from the ocean (Fig. 10(c)) [116]. Inner TENGs are connected in parallel to collect the mechanical energy of the inner liquid under shaking or rotational movement from water waves. A 3D network of TENGs spaced at intervals of 10 cm over a square kilometer could easily generate enough electricity for a town. As shown in Fig. 10(c) [116], the TENG network generates electrical energy and stores it in the capacitor to drive a wireless SOS system that includes a bridge rectifier, a large capacitor, a wireless radio frequency (RF) transmitter, and a receiver. When the voltage of the large capacitor rapidly decreases to about 2.5 V, the RF sensor emits signals that are set as "SOS_SOS_SOS_SOS_."

5.1.4. Integrated marine information detection/signal transmission/display system

Marine environment monitoring is used in a wide range of applications, including water-quality monitoring, ocean sensing, coral reef monitoring, and marine fish farm monitoring, many of which require different wire/wireless sensor networks, system architectures, communication technologies, and sensing technologies. An innovative prototype of a bionic-jellyfish TENG composed of polydimethylsiloxane, polymeric nanocomposite thin film, and metal electrodes has been proposed (Fig. 10(d)) [117]. With a waterproof and adaptive shape, this TENG has an enhanced performance of 143.0 V, 11.8 mA·m^{-2}, and 22.1 l C·m^{-2}, allowing it to directly power green light-emitting diodes (LEDs) or a temperature sensor. The TENG is integrated with a signal-processing circuit,

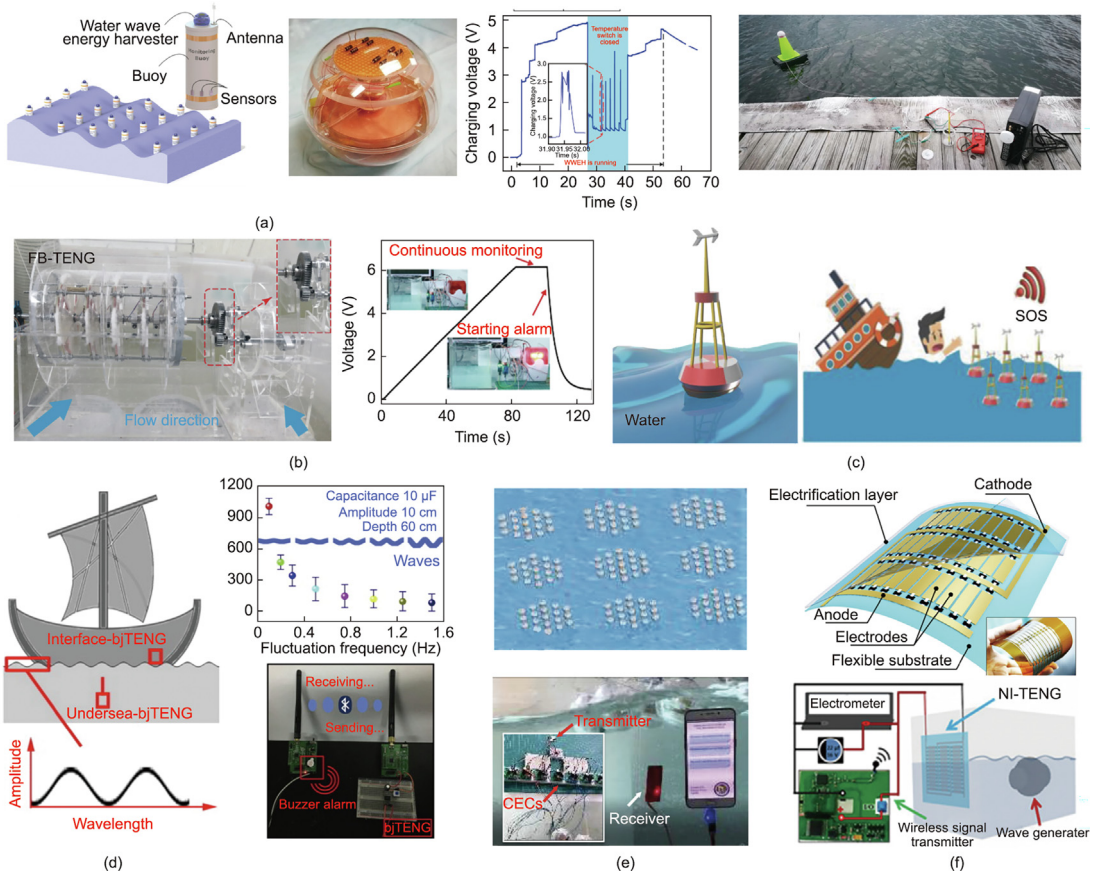

Fig. 10. (a) Schematic illustration of a buoy network for environmental monitoring, with a photo of the TENG structure, a graph showing the performance of the wave-driven temperature alarm system, and a photo of the temperature alarm system in a lake; (b) schematic illustration of a waterwheel-structure TENG for water flow energy harvesting that monitors the weather and gives an alarm when it rains; (c) schematic structure of a TENG-driven buoy with an illustration of its self-powered wireless SOS system for ocean emergencies; (d) workplace scenario of a TENG, with a graph showing the relationship between the early-warning period and fluctuation frequency, and a digital photo of the wireless self-powered fluctuation sensor system; (e) schematic illustration of a TENG network for large-scale blue energy harvesting, with a photo of the transmitted information displayed on a mobile phone screen; (f) schematic illustration of a TENG and wireless signal transmission system. FB-TENG: networked integrated TENG; bjTENG: bionic-jellyfish TENG; NI-TENG: networked integrated TENG. (a) Reproduced from Ref. [34] with permission, (b) reproduced from Ref. [80] with permission, (c) reproduced from Ref. [116] with permission, (d) reproduced from Ref. [117] with permission, (e) reproduced from Ref. [111] with permission, (f) reproduced from Ref. [118] with permission.

constructing a self-powered temperature sensor and wireless self-powered fluctuation early warning system. When the voltage reaches 3 V, the wireless self-powered fluctuation early-warning system triggers a remote controller, which controls a wireless transmitter that can remotely switch a siren between an emergency and a normal state. This TENG can be used to forecast tidal changes and the fluctuation of the sea. As shown in Fig. 10(d) [117], the warning period changes according to the fluctuation frequency of the water, with the warning time being shortened as the fluctuation frequency of the water increases.

A new CEC for TENGs has been developed to harvest water wave energy (Fig. 10(e)) [111]. In this technology, 19 TENG units make up a multi-module TENG network for blue energy harvesting. The charge-excitation TENG network drives a wireless transmitter, which emits signals as the voltage reaches 3 V. The signal is emitted every 20 s and is received and processed by a phone.

A networked integrated TENG has been developed as a highly adaptive means of harvesting energy with various types of water waves (Fig. 10(f)) [118]. The TENG array can adapt to diverse water wave motions and generate a stable electric output. The TENG, which has an area of 100 mm × 70 mm, produces stable electric power of 1.03 mW at a wave height of 12.00 cm, regardless of how random the water waves are. It harvests the dynamic energy of random water waves and power wireless transmitters, thereby showing potential to act as a real-time power supply for environmental pollution detection and even for wireless sensor networks.

5.1.5. Marine positioning system

Marine positioning is the process of using instruments and equipment to determine a ship's position on the ocean and to guide ship navigation, which is important for exploring the ocean. A self-powered seesaw-triboelectric–electromagnetic hybrid nanogenerator has been developed, which harvests energy from water waves with a wide frequency and different directions (Fig. 11(a)) [119]. When the voltage on the global position system (GPS) module reaches 3.3 V, the module is triggered and receives its position from a satellite (Fig. 11(b)) [119]. Next, the GPS module sends the location information to be displayed on a computer screen.

A fully packaged ship-shaped hybrid nanogenerator (SHNG) was developed by Wang et al. [120] to harvest water wave energy using a packaging strategy (Fig. 11(c)). A roller with magnets at both ends continually drives six contact–separation-mode TENGs arranged on the two sides of a ship. This hybrid TENG constitutes a self-powered wireless positioning system to locate the position of the water source. The GPS module can be continuously powered to send wireless signals in a timely manner. These TENGs can be integrated into networks to harvest water wave energy effectively, offering the advantage of a multi-source location while facilitating the provision of drinking water.

5.2. Self-powered ocean sensors

The development of TENG technology lays a foundation for the construction of self-powered marine environmental application systems, which have great significance for human production and life.

5.2.1. Ocean-wave spectrum sensor

A performance-enhanced rolling TENG based on a movable part and two stationary films was developed by Chen et al. [121] in 2021 (Fig. 12(a)). In the rolling TENG, the contact/separation of the rolling ball and the triboelectric layer drives an electron flow and produces electricity. The output voltage changes with the amplitude and frequency of the waves. The output voltages of the TENG are 4.8, 7.1, and 8.5 V at amplitudes of 10, 20, and 30 cm, respectively. When the typical water wave amplitude is 20 cm, the TENG's output voltage increases with the water wave frequency.

5.2.2. Water/liquid level sensor

A magnetic flap-type difunctional sensor based on a TENG has been developed to detect pneumatic flow and liquid levels [27].

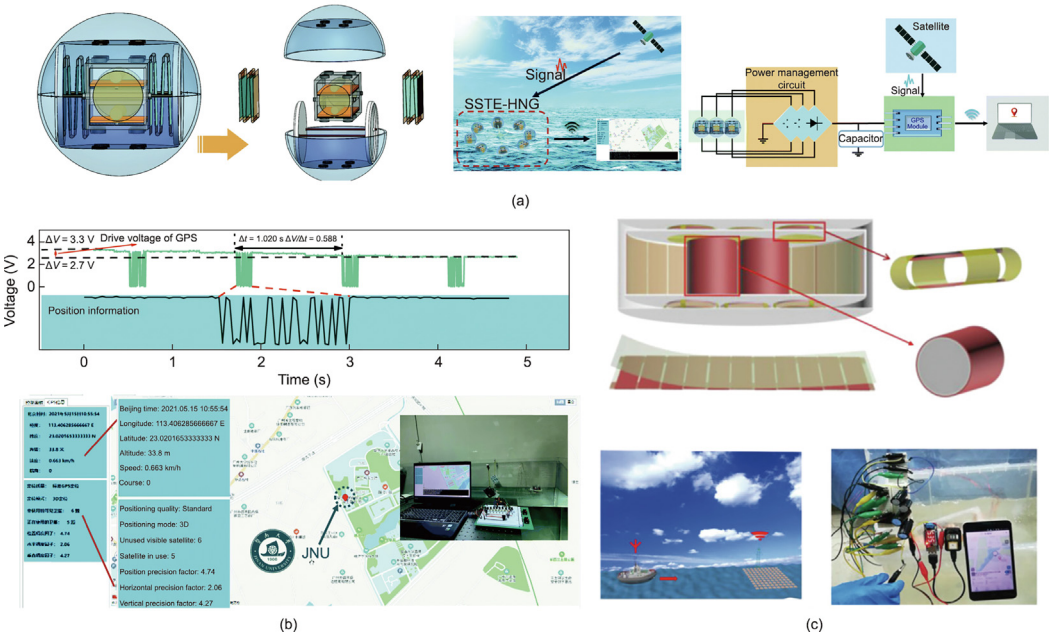

Fig. 11. Marine positioning system. (a) Schematic diagrams of the designed TENG and its application in sea surface wireless positioning. A flow chart shows the global position system (GPS) module being driven through a transistor-controlled power management circuit. (b) Computer interface of the located position. (c) Schematic diagram of the designed SHNG and its self-powered wireless positioning system, and an application demonstration of driving the GPS module. SSTE-HNG: structured spherical triboelectric–electromagnetic hybrid nanogenerator; JNU: Jinan University. (a,b) Reproduced from Ref. [119] with permission, (c) reproduced from Ref. [120] with permission.

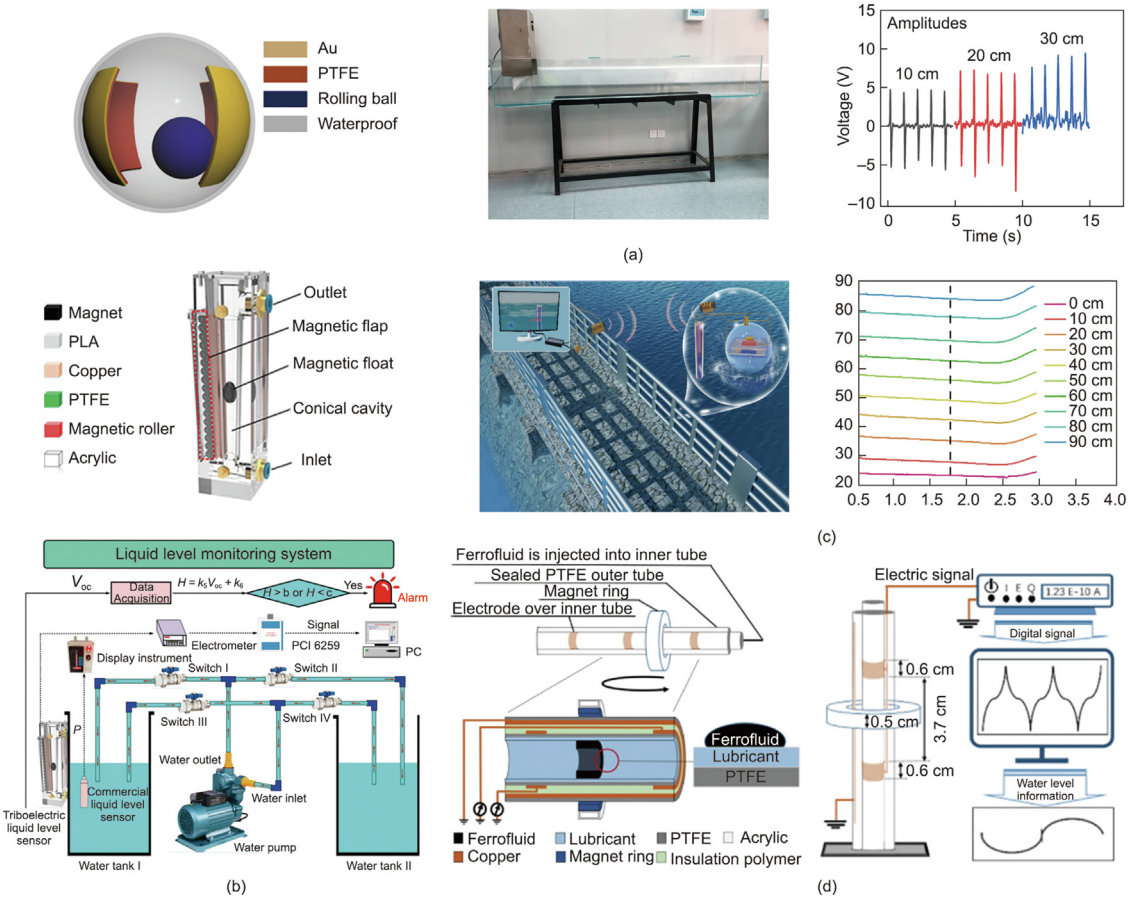

Fig. 12. (a) Schematic structure of a TENG, with a photo of the designed wave pool, and a graph showing the output voltages under different wave amplitudes. (b) Schematic diagrams of a magnetic flap-type difunctional sensor and liquid-level parameter detection. (c) Schematic diagrams of a TENG-based self-powered wireless liquid sensor system. (d) Schematic of a magnetic-field-assisted non-contact TENG and its detection process as a water-level sensor. V_{oc}: the open-circuit voltage; k_5 and k_6 the open-circuit voltage; $k5$ and $k6$: constant coefficients; PC: personal computer. (a) Reproduced from Ref. [121] with permission. (b) Reproduced from Ref. [27] with permission. (c) Reproduced from Ref. [122] with permission. (d) Reproduced from Ref. [123] with permission.

This TENG consists of an outer magnetic flap, a magnetic float, and a conical cavity. As shown in Fig. 12(b) [27], the simulated water-level test-cycle system consists of a pump and a series of water pipes. The rise and fall of the water level are controlled by the four switches. For example, when switches I and IV are on and switches II and III are off, the water level in water tank I rises. Moreover, the switch can control the rise and fall rates of the water level. An alarm response is triggered if the liquid level is lower or higher than a set value.

In 2022, Xu et al. [122] developed a cylindrical type of liquid level sensor based on a TENG that uses a small ferric magnetic core for the transmission coils (Fig. 12(c)). An impedance analyzer is used to measure the capacitances of the sensor under 500 kHz and 3 MHz. The sensor responds to the liquid level, which monitors the liquid level in a timely manner. Along with the wireless liquid-level sensor, the resonant frequency and signal amplitude change with the liquid level.

A novel magnetic-field-assisted non-contact TENG has been developed that drives the motion of a ferrofluid under an external magnetic field without direct contact [123]. With a lubricant oil layer, this TENG is immersed in the water in a glass pot with a valve and vertically fixed over a stage. The width of the electrode, the distance between electrodes, and the thickness of the magnet ring are labeled, as shown in Fig. 12(d) [123]. The motion of the magnet ring drives the motion of the ferrofluid along with the water level, which causes electron transfer to occur on the electrode. Water level information is then acquired via electric signal change.

5.3. Underwater wireless communication

With the vigorous development of marine exploration, the improvement of underwater equipment and technology has attracted increasing attention. Underwater wireless communication has always been critical for understanding and developing the ocean. At present, underwater communication is realized through various physical fields such as sound, light, and electromagnetic fields. Because sound waves are not easily absorbed by water, unlike electromagnetic waves and light waves easily absorbed by water, underwater acoustic communication has become the most widely used underwater communication method. However, underwater acoustic communication is accompanied by considerable transmission delay, and the transmission is affected by temperature, pressure, and salinity. In contrast to sound and light waves, electromagnetic waves are immune to noise and turbulence. Underwater displacement current communication has the typical characteristics of a high transmission rate and low delay. High-frequency electromagnetic waves are mainly absorbed by water, while low-frequency electromagnetic waves can be transmitted through antennas several kilometers long.

This paper applies TENG technology to underwater wireless communication for the first time, innovatively realizing self-powered underwater wireless signal transmission in complex waters (Fig. 13(a)) [41]. The research team deeply analyzed the transmission mechanism of underwater electric field signals from the perspective of Maxwell's displacement current, built an underwater wireless communication experimental system, and con-

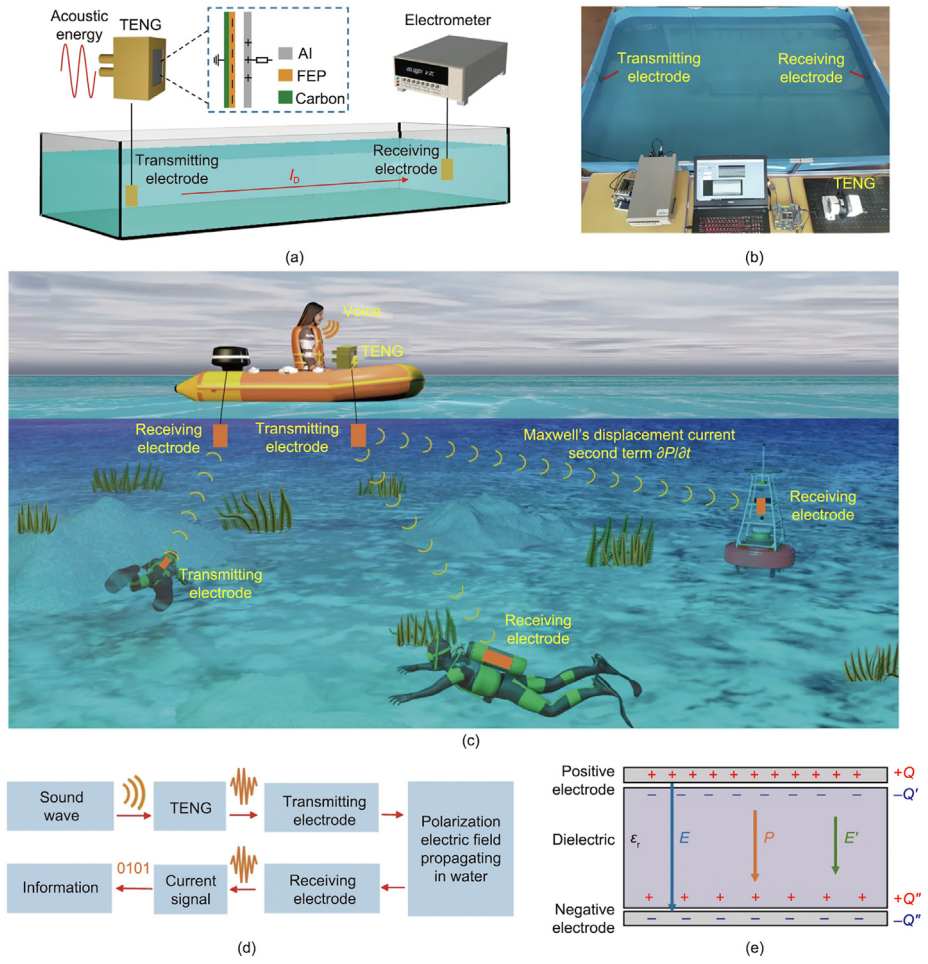

Fig. 13. Underwater wireless communication via a TENG-generated Maxwell displacement current. (a) Schematic diagram and (b) photo of the experimental process; (c) schematic diagram of underwater electric field communication application based on a TENG; (d) flow chart of underwater wireless communication; (e) schematic diagram of the capacitance model. ε_r: relative permittivity; ***E***: the original electric field; ***P***: the polarization electric field; ***E′***: the combined electric field of ***E*** and ***P***; Q: amount of charge. Reproduced from Ref. [41] with permission.

ducted many experiments (Figs. 13(b) and (c)) [41]. The experimental results show that the underwater electric field signal is not disturbed by salinity, turbidity, and underwater obstacles, and that its waveform will not be distorted even through a 100 m long spiral water pipe (Fig. 13(d)) [41]. This new underwater electric field communication method based on a TENG technology has the advantages of having a stable signal, being unaffected by obstacles, and being self-supplied. Moreover, the TENG's current signals exhibit good anti-interference ability when encountering underwater disturbances. The peak value of the current signal decreased by 66% compared with the original signal and the waveform of the electrical signal was not distorted as the signal passed through a 100 m long saltwater pipe (Fig. 13(e)) [41]. Text and images can be successfully transmitted in the tank by utilizing on/off keying. No error was found in the continuous transmission of about 20 000 digital signals, and the underwater lighting system has wireless voice control via the TENG.

5.4. Self-powered electrochemical system

The service lives of offshore facilities and equipment are shortened by metal corrosion, leading to great economic losses. A segmented swing-structured fur-based TENG has been designed and fabricated to provide a self-powered solution for impressed current cathodic protection (Fig. 14(a)) [124]. Polished Q235 carbon steel as the cathode and graphite sheet as the anode are immersed in a 3.5% NaCl solution. The results show that the corrosion of carbon steel can be reduced and retarded with a metal corrosion-protection system.

A self-powered electrochemical system based on a TENG was designed by Feng et al. [125] for the conversion of water wave energy to green energy in the form of hydrogen fuel (Fig. 14(b)). The self-powered electrochemical system consists of a TENG network, an energy storage module, an electrolyzer, feeding equipment, and terminal gasometers and tanks. The self-powered electrochemical system generates H_2 fuel at a rate of 814.8 $\mu L \cdot m^{-2} \cdot d^{-1}$ with a Faraday efficiency of 69.1% and a conversion efficiency of 44.3%, under ideal conditions.

TENG-based durable superhydrophobic fluorinated silica (F-SiO_2)/epoxy resin (FE) coatings with good corrosion resistance were developed by Liu et al. [126] to fabricate a synergistic anti-corrosion system for self-powered cathodic protection (Fig. 14(c)). In a 3.5 wt% NaCl solution, the corrosion potential (E_{corr}) of an Al sheet protected by the synergistic anti-corrosion system was found to dramatically decrease by 745 mV.

A marine self-charging power system based on a seawater supercapacitor and a TENG module has been developed (Fig. 14(d)) [127]. Due to its hollow design, the electrode exhibits

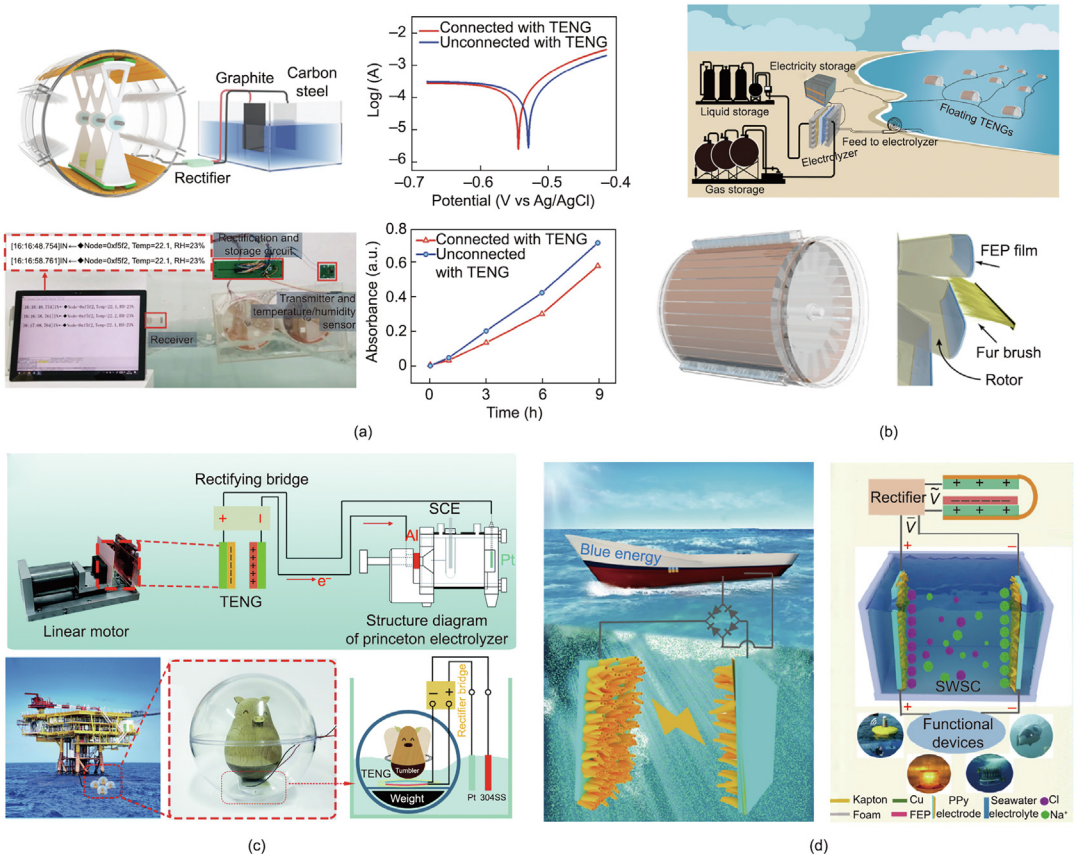

Fig. 14. (a) Schematic diagram of a simulated metal protection system and a remote marine environmental information monitoring system, with the Tafel curves of Q235 carbon steel and the absorption intensity of Fe^{3+} ions leached from NaCl solution. (b) Schematic diagram of a self-powered electrochemical system and TENG. (c) Schematic illustration of a linear motor-driven synergistic corrosion–protection system. Self-powered cathodic protection is carried out by collecting wave energy through spherical TENGs connected in series. (d) Schematic diagram of the structural design and working mechanism of a self-charging marine power system. PPy: polypyrrole. (a) Reproduced from Ref. [124] with permission, (b) reproduced from Ref. [125] with permission, (c) reproduced from Ref. [126] with permission, (d) reproduced from Ref. [127] with permission.

improved stability and capacitance, achieving a high power density of 4.32 $kW{\cdot}kg^{-1}$ under an energy density of 5.12 $W{\cdot}h{\cdot}kg^{-1}$. The TENG module can harvest water wave energy to realize a self-charging marine power system that can power electronics and sensors, displaying competitive potential for the smart ocean and Internet of Things.

6. Conclusions and prospects

This paper reviewed the advances of TENGs for blue energy harvesting and marine environmental monitoring. First, it introduced the theoretical foundations of TENGs, including their fundamental physics mechanisms and working modes, and the original idea of using TENG networks to harvest large-scale blue energy. Next, it elaborated on related progress in advanced TENG prototypes for improving the efficiency, durability, and applications of TENGs in blue energy harvesting, such as the rolling-ball, rotating-disk, 3D electrode, spring-assisted, mass-spring, and pendulum-like structures. Moreover, it discussed performance enhancement strategies for TENGs in blue energy harvesting. Material and structural optimization has dramatically improved the output of TENGs in the literature, while power management and charge excitation are promising ways to enhance TENG performance in the future. Finally, this review summarized marine environmental applications of TENGs based on blue energy harvesting, including applications in powering distributed sensors and signal transmission systems in the ocean, serving as self-powered sensors in the sea, and constructing self-powered electrochemical systems. Table 2 [77–93] summarizes a performance comparison of different TENG prototypes for blue energy harvesting.

The use of millions of TENG units to construct 3D TENG networks holds the possibility of realizing the dream of large-scale blue energy harvesting [40]. One TENG unit can generate a power of about 10 mW, with a power density of up to 10 $W{\cdot}m^{-3}$ under a water wave of two or three times per second. A TENG network covering an ocean area equal to the size of Georgia and having a depth of 10 m can produce a power of 16 TW, which meets the world's annual total energy needs. Meanwhile, other energy harvesting devices can be hybridized with the TENG networks to achieve the synergistic energy harvesting of water waves, wind, and solar energy. The electricity produced could be used locally on a floating platform or transferred to power plants or the grid on land. The development of ocean blue energy will provide a new paradigm for carbon neutrality. If the dream of blue energy can be realized, the ensuing social and economic effects will be immeasurable, and an energy revolution may be induced, vigorously promoting the development of social productivity and the progress of human civilization.

Challenges remain to be addressed before large-scale TENG networks can be achieved and further progress can be made toward the blue energy dream. For example, the TENG energy harvesting efficiency, device durability, networking design, and application expansion still require further research. We suggest the following key areas as the focus of future investigations:

Table 2
Performance comparison of different TENG prototypes for blue energy harvesting.

TENG type	Structure	Peak power (mW)	Peak power density ($W·m^{-2}$)	Test environment	Ref.
Rolling-structured, freestanding	Rolling-ball	10	—	No	[77]
Duck-shaped TENG	Rolling-ball structure	7.64	0.455	Water waves	[78]
TS	Rolling-ball structure	0.07	0.21	No	[79]
Fur-brush TENG	Rotating-disk structure	56.79	5.02	No	[80]
TD	Rotating-disk structure	29.4	7.3 $W·m^{-3}$	No	[81]
Robust swing-structured	Swing-structured	4.56	1.29 $W·m^{-3}$	No	[82]
Cylindrical	Swing-structured	0.11	0.23 $W·m^{-3}$	Water waves	[83]
3D electrodes	3D electrode	8.75	32.6 $W·m^{-3}$	Water waves	[84]
Spring-assisted	Spring-assisted structure	5.38	—	No	[85]
Spring-assisted swing	Spring-assisted structure	4.1	—	Water waves	[86]
Helical TENG	Spring-assisted structure	—	240 (under vertical resonance vibration, 16 Hz); 45 (horizontal resonance vibration, 8.5 Hz)	Resonance vibration of 23 $m·s^{-2}$	[87]
Multilayered	Mass-spring structure	—	—	No	[88]
Multilayered	Multilayered structure	15.97	15.2 $W·m^{-3}$	No	[89]
Spring-assisted multilayered	Multilayered structure	—	0.26	No	[90]
Pendulum-like component	Pendulum-like structure	0.028	—	No	[91]
Hybrid TENG	Pendulum-like structure	1.72	0.41	No	[92]
Hybrid TENG	Pendulum-like structure	530	—	No	[93]

(1) Developing power management and storage technologies for different types of TENGs to enhance performance;
(2) Designing other energy units to raise the harvesting capacity of ocean energy;
(3) Improving the durability and reducing the corrosion of TENG systems to ensure reliability and long lifetime;
(4) Developing a variety of ocean-related self-powered system applications.

TENGs will soon achieve breakthroughs in ocean equipment power supply, island power supply, marine navigation and positioning, and underwater or water surface monitoring, so the blue energy dream is bound to come true.

Author's contribution

Yang Jiang: original draft, Writing. Xi Liang: original draft, Writing. Tao Jiang: Visualization. Zhong Lin Wang: Visualization.

Compliance with ethics guidelines

Yang Jiang, Xi Liang, Tao Jiang, and Zhong Lin Wang declare that they have no conflict of interest or financial conflicts to disclose.

Acknowledgments

The authors thank the National Key Research and Development Project from the Minister of Science and Technology (2021YFA1201601 and 2021YFA1201604), the Innovation Project of Ocean Science and Technology (22-3-3-hygg-18-hy), the project supported by the Fundamental Research Funds for the Central Universities (E2E46805), the China National Postdoctoral Program for Innovative Talents (BX20220292), and the China Postdoctoral Science Foundation (2022M723100).

Compliance with ethics guidelines

Yang Jiang, Xi Liang, Tao Jiang, and Zhong Lin Wang declare that they have no conflict of interest or financial conflicts to disclose.

References

[1] Boccotti P. On a new wave energy absorber. Ocean Eng 2003;30(9):1191–200.
[2] Guo Y, Han Q, Wang J, Yu X. Energy-aware localization algorithm for ocean Internet of Things. Sens Rev 2018;38(2):129–36.
[3] Kröger S, Law RJ. Sensing the sea. Trends Biotechnol 2005;23(5):250–6.
[4] Falnes J. A review of wave-energy extraction. Mar Structures 2007;20(4):185–201.
[5] Khojasteh D, Kamali R. Evaluation of wave energy absorption by heaving point absorbers at various hot spots in Iran seas. Energy 2016;109:629–40.
[6] Lu H, Wang D, Li Y, Li J, Li X, Kim H, et al. CONet: a cognitive ocean network. IEEE Wirel Commun 2019;26(3):90–6.
[7] Marcelli M, Piermattei V, Madonia A, Mainardi U. Design and application of new low-cost instruments for marine environmental research. Sensors (Basel) 2014;14(12):23348–64.
[8] Sudhakar M, Trishul A, Doble M, Suresh Kumar K, Syed Jahan S, Inbakandan D, et al. Biofouling and biodegradation of polyolefins in ocean waters. Polym Degrad Stabil 2007;92(9):1743–52.
[9] Wu N, Wang Q, Xie X. Ocean wave energy harvesting with a piezoelectric coupled buoy structure. Appl Ocean Res 2015;50:110–8.
[10] Yang J, Wen J, Wang Y, Jiang B, Wang H, Song H. Fog-based marine environmental information monitoring toward ocean of things. IEEE Internet Things 2020;7(5):4238–47.
[11] Zheng C, Shao L, Shi W, Su Q, Lin G, Li X, et al. An assessment of global ocean wave energy resources over the last 45 a. Acta Oceanol Sin 2014;33(1):92–101.
[12] Borthwick AGL. Marine renewable energy seascape. Engineering 2016;2(1):69–78.
[13] Callow JA, Callow ME. Trends in the development of environmentally friendly fouling-resistant marine coatings. Nat Commun 2011;2(1):244.
[14] Chaplin RV. Seaweaver: a new surge-resonant wave energy converter. Renew Energy 2013;57:662–70.
[15] Chen H, Tang T, Ait-Ahmed N, Benbouzid MEH, Machmoum M, Zaim MEH. Attraction, challenge and current status of marine current energy. IEEE Access 2018;6:12665.
[16] Heath TV. A review of oscillating water columns. Philos Trans Royal Soc 1959;2012(370):235–45.
[17] Kwon SD, Park J, Law K. Electromagnetic energy harvester with repulsively stacked multilayer magnets for low frequency vibrations. Smart Mater Struct 2013;22(5):055007.
[18] Lai YC, Hsiao YC, Wu HM, Wang ZL. Waterproof fabric-based multifunctional triboelectric nanogenerator for universally harvesting energy from raindrops, wind, and human motions and as self-powered sensors. Adv Sci (Weinh) 2019;6(5):1801883.
[19] Leijon M, Danielsson O, Eriksson M, Thorburn K, Bernhoff H, Isberg J, et al. An electrical approach to wave energy conversion. Renew Energy 2006;31(9):1309–19.
[20] Lucas A, Pinkel R, Alford M. Ocean wave energy for long endurance, broad bandwidth ocean monitoring. Oceanography 2017;30(2):126–7.
[21] Luo J, Wang ZL. Recent advances in triboelectric nanogenerator based self-charging power systems. Energy Storage Mater 2019;23:617–28.
[22] Melikoglu M. Current status and future of ocean energy sources: a global review. Ocean Eng 2018;148:563–73.
[23] Moretti G, Santos Herran M, Forehand D, Alves M, Jeffrey H, Vertechy R, et al. Advances in the development of dielectric elastomer generators for wave energy conversion. Renew Sustain Energy Rev 2020;117:109430.
[24] Mueller P, Thoss H, Kaempf L, Güntner A. A buoy for continuous monitoring of suspended sediment dynamics. Sensors (Basel) 2013;13(10):13779–801.
[25] Mutsuda H, Tanaka Y, Patel R, Doi Y. Harvesting flow-induced vibration using a highly flexible piezoelectric energy device. Appl Ocean Res 2017;68:39–52.
[26] Wang X, Shang J, Luo Z, Tang L, Zhang X, Li J. Reviews of power systems and environmental energy conversion for unmanned underwater vehicles. Renew Sustain Energy Rev 2012;16(4):1958–70.

[27] Wang Z, Yu Y, Wang Y, Lu X, Cheng T, Bao G, et al. Magnetic flap-type difunctional sensor for detecting pneumatic flow and liquid level based on triboelectric nanogenerator. ACS Nano 2020;14(5):5981–7.
[28] Zhao T, Xu M, Xiao X, Ma Y, Li Z, Wang ZL. Recent progress in blue energy harvesting for powering distributed sensors in ocean. Nano Energy 2021;88:106199.
[29] Yurchenko D, Alevras P. Parametric pendulum based wave energy converter. Mech Syst Signal Process 2018;99:504–15.
[30] Domingo MC. An overview of the internet of underwater things. J Netw Comput Appl 2012;35(6):1879–90.
[31] Martínez-Vicente V, Clark JR, Corradi P, Aliani S, Arias M, Bochow M, et al. Measuring marine plastic debris from space: initial assessment of observation requirements. Remote Sens (Basel) 2019;11(20):2443.
[32] Xu G, Shen W, Wang X. Applications of wireless sensor networks in marine environment monitoring: a survey. Sensors (Basel) 2014;14(9):16932–54.
[33] Shao H, Cheng P, Chen R, Xie L, Sun N, Shen Q, et al. Triboelectric–electromagnetic hybrid generator for harvesting blue energy. Nano–Micro Lett 2018;10(3):54.
[34] Wu Z, Guo H, Ding W, Wang YC, Zhang L, Wang ZL. A hybridized triboelectric-electromagnetic water wave energy harvester based on a magnetic sphere. ACS Nano 2019;13(2):2349–56.
[35] Cheng P, Guo H, Wen Z, Zhang C, Yin X, Li X, et al. Largely enhanced triboelectric nanogenerator for efficient harvesting of water wave energy by soft contacted structure. Nano Energy 2019;57:432–9.
[36] Zhang W, Shi Y, Li Y, Chen X, Shen H. A review: contact electrification on special interfaces. Front Mater 2022;9:909746.
[37] Fan FR, Tian ZQ, Lin WZ. Flexible triboelectric generator. Nano Energy 2012;1(2):328–34.
[38] Wang ZL. Triboelectric nanogenerators as new energy technology and self-powered sensors-principles, problems and perspectives. Faraday Discuss 2014;176:447–58.
[39] Wang ZL. Triboelectric nanogenerator (TENG)—sparking an energy and sensor revolution. Adv Energy Mater 2020;10(17):2000137.
[40] Wang ZL, Jiang T, Xu L. Toward the blue energy dream by triboelectric nanogenerator networks. Nano Energy 2017;39:9–23.
[41] Zhao H, Xu M, Shu M, An J, Ding W, Liu X, et al. Underwater wireless communication via TENG-generated Maxwell's displacement current. Nat Commun 2022;13(1):3325.
[42] Vu DL, Vo CP, Le CD, Ahn KK. Enhancing the output performance of fluid-based triboelectric nanogenerator by using poly (vinylidene fluoride-co-hexafluoropropylene)/ionic liquid nanoporous membrane. Int J Energy Res 2021;45:8960.
[43] Fang C, Tong T, Bu T, Cao Y, Xu S, Qi Y, et al. Overview of power management for triboelectric nanogenerators. Adv Intell Syst-Ger 2020;2(2):1900129.
[44] Wang ZL. On Maxwell's displacement current for energy and sensors: the origin of nanogenerators. Mater Today 2017;20(2):74–82.
[45] Wang ZL. Entropy theory of distributed energy for internet of things. Nano Energy 2019;58:669–72.
[46] Wang H, Xu L, Wang Z. Advances of high-performance triboelectric nanogenerators for blue energy harvesting. Nanoenergy Adv 2021;1(1):32–57.
[47] Huang B, Wang P, Wang L, Yang S, Wu D. Recent advances in ocean wave energy harvesting by triboelectric nanogenerator: an overview. Nanotechnol Rev 2020;9(1):716–35.
[48] Xi F, Pang Y, Li W, Jiang T, Zhang L, Guo T, et al. Universal power management strategy for triboelectric nanogenerator. Nano Energy 2017;37:168–76.
[49] Ellabban O, Abu-Rub H, Blaabjerg F. Renewable energy resources: current status, future prospects and their enabling technology. Renew Sustain Energy Rev 2014;39:748–64.
[50] Henderson R. Design, simulation, and testing of a novel hydraulic power take-off system for the Pelamis wave energy converter. Renew Energy 2006;31(2):271–83.
[51] Liang X, Jiang T, Liu G, Xiao T, Xu L, Li W, et al. Triboelectric nanogenerator networks integrated with power management module for water wave energy harvesting. Adv Funct Mater 2019;29(41):1807241.
[52] Xu W, Li X, Brugger J, Liu X. Study of the enhanced electricity output of a sliding droplet-based triboelectric nanogenerator for droplet sensor design. Nano Energy 2022;98:107166.
[53] Yang HM, Deng MM, Tang Q, He WC, Hu CG, Xi Y, et al. A nonencapsulative pendulum-like paper-based hybrid nanogenerator for energy harvesting. Adv Energy Mater 2019;9(33):1901149.
[54] Ying Z, Long Y, Yang F, Dong Y, Li J, Zhang Z, et al. Self-powered liquid chemical sensors based on solid–liquid contact electrification. Analyst (Lond) 2021;146(5):1656–62.
[55] Zhang C, Zhang B, Yuan W, Yang O, Liu Y, He L, et al. Seawater-based triboelectric nanogenerators for marine anticorrosion. ACS Appl Mater Interfaces 2022;14(6):8605–12.
[56] Zheng Q, Shi B, Fan F, Wang X, Yan L, Yuan W, et al. *In vivo* powering of pacemaker by breathing-driven implanted triboelectric nanogenerator. Adv Mater 2014;26(33):5851–6.
[57] Zhou H, Dong J, Liu H, Zhu L, Xu C, He X, et al. The coordination of displacement and conduction currents to boost the instantaneous power output of a water-tube triboelectric nanogenerator. Nano Energy 2022;95:107050.
[58] Chen H, Xing C, Li Y, Wang J, Xu Y. Triboelectric nanogenerators for a macro-scale blue energy harvesting and self-powered marine environmental monitoring system. Sustain Energy Fuels 2020;4(3):1063–77.
[59] Xu C, Zhang B, Wang AC, Zou H, Liu G, Ding W, et al. Contact-electrification between two identical materials: curvature effect. ACS Nano 2019;13(2):2034–41.
[60] Yi F, Lin L, Niu S, Yang J, Wu W, Wang S, et al. Self-powered trajectory, velocity, and acceleration tracking of a moving object/body using a triboelectric sensor. Adv Funct Mater 2014;24(47):7488–94.
[61] Zhang H, Yang Y, Su Y, Chen J, Adams K, Lee S, et al. Triboelectric nanogenerator for harvesting vibration energy in full space and as self-powered acceleration sensor. Adv Funct Mater 2014;24(10):1401–7.
[62] Zhang X, Zheng Y, Wang D, Rahman ZU, Zhou F. Liquid–solid contact triboelectrification and its use in self-powered nanosensor for detecting organics in water. Nano Energy 2016;30:321–9.
[63] Zhu G, Bai P, Chen J, Lin WZ. Power-generating shoe insole based on triboelectric nanogenerators for self-powered consumer electronics. Nano Energy 2013;2(5):688–92.
[64] Zhu G, Lin ZH, Jing Q, Bai P, Pan C, Yang Y, et al. Toward large-scale energy harvesting by a nanoparticle-enhanced triboelectric nanogenerator. Nano Lett 2013;13(2):847–53.
[65] Zhu G, Chen J, Liu Y, Bai P, Zhou YS, Jing Q, et al. Linear-grating triboelectric generator based on sliding electrification. Nano Lett 2013;13(5):2282–9.
[66] Zhu M, He T, Lee C. Technologies toward next generation human machine interfaces: from machine learning enhanced tactile sensing to neuromorphic sensory systems. Appl Phys Rev 2020;7(3):031305.
[67] Zi Y, Niu S, Wang J, Wen Z, Tang W, Wang ZL. Standards and figure-of-merits for quantifying the performance of triboelectric nanogenerators. Nat Commun 2015;6(1):8376.
[68] Zou H, Zhang Y, Guo L, Wang P, He X, Dai G, et al. Quantifying the triboelectric series. Nat Commun 2019;10(1):1427.
[69] Xue H, Yang Q, Wang D, Luo W, Wang W, Lin M, et al. A wearable pyroelectric nanogenerator and self-powered breathing sensor. Nano Energy 2017;38:147–54.
[70] Zhu G, Zhou YS, Bai P, Meng XS, Jing Q, Chen J, et al. A shape-adaptive thin-film-based approach for 50% high-efficiency energy generation through micro-grating sliding electrification. Adv Mater 2014;26(23):3788–96.
[71] Wang ZL. From contact electrification to triboelectric nanogenerators. Rep Prog Phys 2021;84(9):096502.
[72] Xu L, Jiang T, Lin P, Shao JJ, He C, Zhong W, et al. Coupled triboelectric nanogenerator networks for efficient water wave energy harvesting. ACS Nano 2018;12(2):1849–58.
[73] Wang ZL. On the first principle theory of nanogenerators from Maxwell's equations. Nano Energy 2020;68:104272.
[74] Wang ZL. On the expanded Maxwell's equations for moving charged media system-general theory, mathematical solutions and applications in TENG. Mater Today 2022;52:348–63.
[75] Wang ZL. The expanded Maxwell's equations for a mechano-driven media system that moves with acceleration. Int J Mod Phys B 2023;37(16):2350159.
[76] Zhang C, Tang W, Han C, Fan F, Wang ZL. Theoretical comparison, equivalent transformation, and conjunction operations of electromagnetic induction generator and triboelectric nanogenerator for harvesting mechanical energy. Adv Mater 2014;26(22):3580–91.
[77] Wang X, Niu S, Yin Y, Yi F, You Z, Wang ZL. Triboelectric nanogenerator based on fully enclosed rolling spherical structure for harvesting low-frequency water wave energy. Adv Energy Mater 2015;5(24):1501467.
[78] Ahmed A, Saadatnia Z, Hassan I, Zi Y, Xi Y, He X, et al. Self-powered wireless sensor node enabled by a duck-shaped triboelectric nanogenerator for harvesting water wave energy. Adv Energy Mater 2017;7(7):1601705.
[79] Liu W, Xu L, Bu T, Yang H, Liu G, Li W, et al. Torus structured triboelectric nanogenerator array for water wave energy harvesting. Nano Energy 2019;58:499–507.
[80] Chen P, An J, Shu S, Cheng R, Nie J, Jiang T, et al. Super-durable, low-wear, and high-performance fur-brush triboelectric nanogenerator for wind and water energy harvesting for smart agriculture. Adv Energy Mater 2021;11(9):2003066.
[81] Bai Y, Xu L, He C, Zhu L, Yang X, Jiang T, et al. High-performance triboelectric nanogenerators for self-powered, *in-situ* and real-time water quality mapping. Nano Energy 2019;66:104117.
[82] Jiang T, Pang H, An J, Lu P, Feng Y, Liang X, et al. Robust swing-structured triboelectric nanogenerator for efficient blue energy harvesting. Adv Energy Mater 2020;10(23):2000064.
[83] Feng Y, Liang X, An J, Jiang T, Wang ZL. Soft-contact cylindrical triboelectric-electromagnetic hybrid nanogenerator based on swing structure for ultra-low frequency water wave energy harvesting. Nano Energy 2021;81:105625.
[84] Yang X, Xu L, Lin P, Zhong W, Bai Y, Luo J, et al. Macroscopic self-assembly network of encapsulated high-performance triboelectric nanogenerators for water wave energy harvesting. Nano Energy 2019;60:404–12.
[85] Jiang T, Yao Y, Xu L, Zhang L, Xiao T, Wang ZL. Spring-assisted triboelectric nanogenerator for efficiently harvesting water wave energy. Nano Energy 2017;31:560–7.
[86] Liang X, Liu Z, Feng Y, Han J, Li L, An J, et al. Spherical triboelectric nanogenerator based on spring-assisted swing structure for effective water wave energy harvesting. Nano Energy 2021;83:105836.

[87] Xu M, Wang P, Wang YC, Zhang SL, Wang AC, Zhang C, et al. A soft and robust spring based triboelectric nanogenerator for harvesting arbitrary directional vibration energy and self-powered vibration sensing. Adv Funct Mater 2018;8(9):1702432.
[88] Xi F, Pang Y, Liu G, Wang S, Li W, Zhang C, et al. Self-powered intelligent buoy system by water wave energy for sustainable and autonomous wireless sensing and data transmission. Nano Energy 2019;61:1–9.
[89] Xiao TX, Liang X, Jiang T, Xu L, Shao JJ, Nie JH, et al. Spherical triboelectric nanogenerators based on spring-assisted multilayered structure for efficient water wave energy harvesting. Adv Funct Mater 2018;28(35):1802634.
[90] Chen J, Yang J, Li Z, Fan X, Zi Y, Jing Q, et al. Networks of triboelectric nanogenerators for harvesting water wave energy: a potential approach toward blue energy. ACS Nano 2015;9(3):3324–31.
[91] Lin Z, Zhang B, Xie Y, Wu Z, Yang J, Wang ZL. Elastic-connection and soft-contact triboelectric nanogenerator with superior durability and efficiency. Adv Funct Mater 2021;31(40):2105237.
[92] Ren Z, Liang X, Liu D, Li X, Ping J, Wang Z, et al. Water-wave driven route avoidance warning system for wireless ocean navigation. Adv Energy Mater 2021;11(31):2101116.
[93] Xie W, Gao L, Wu L, Chen X, Wang F, Tong D, et al. A nonresonant hybridized electromagnetic-triboelectric nanogenerator for irregular and ultralow frequency blue energy harvesting. Research 2021;2021:5963293.
[94] Zhang XS, Han MD, Meng B, Zhang HX. High performance triboelectric nanogenerators based on large-scale mass-fabrication technologies. Nano Energy 2015;11:304–22.
[95] Zou H, Guo L, Xue H, Zhang Y, Shen X, Liu X, et al. Quantifying and understanding the triboelectric series of inorganic non-metallic materials. Nat Commun 2020;11(1):2093.
[96] Hou C, Chen T, Li Y, Huang M, Shi Q, Liu H, et al. A rotational pendulum based electromagnetic/triboelectric hybrid-generator for ultra-low-frequency vibrations aiming at human motion and blue energy applications. Nano Energy 2019;63:103871.
[97] Chen X, Gao L, Chen J, Lu S, Zhou H, Wang T, et al. A chaotic pendulum triboelectric-electromagnetic hybridized nanogenerator for wave energy scavenging and self-powered wireless sensing system. Nano Energy 2020;69:104440.
[98] Wang JY, Pan L, Guo HY, Zhang BB, Zhang RR, Wu ZY, et al. Rational structure optimized hybrid nanogenerator for highly efficient water wave energy harvesting. Adv Energy Mater 2019;9(8):1802892.
[99] Tian S, Wei X, Lai L, Li B, Wu Z, Dai Y. Frequency modulated hybrid nanogenerator for efficient water wave energy harvesting. Nano Energy 2022;102:107669.
[100] Zhu Z, Xiang H, Zeng Y, Zhu J, Cao X, Wang N, et al. Continuously harvesting energy from water and wind by pulsed triboelectric nanogenerator for self-powered seawater electrolysis. Nano Energy 2022;93:106776.
[101] Zhang Q, Liang Q, Nandakumar DK, Qu H, Shi Q, Alzakia FI, et al. Shadow enhanced self-charging power system for wave and solar energy harvesting from the ocean. Nat Commun 2021;12(1):616.
[102] Wang ZL. Catch wave power in floating nets. Nature 2017;542(7640):159–60.
[103] Xu M, Zhao T, Wang C, Zhang SL, Li Z, Pan X, et al. High power density tower-like triboelectric nanogenerator for harvesting arbitrary directional water wave energy. ACS Nano 2019;13(2):1932–9.
[104] Zhang SL, Xu M, Zhang C, Wang YC, Zou H, He X, et al. Rationally designed sea snake structure based triboelectric nanogenerators for effectively and efficiently harvesting ocean wave energy with minimized water screening effect. Nano Energy 2018;48:421–9.
[105] Cheng L, Xu Q, Zheng Y, Jia X, Qin Y. A self-improving triboelectric nanogenerator with improved charge density and increased charge accumulation speed. Nat Commun 2018;9(1):3773.
[106] Xu L, Bu TZ, Yang XD, Zhang C, Wang ZL. Ultrahigh charge density realized by charge pumping at ambient conditions for triboelectric nanogenerators. Nano Energy 2018;49:625–33.
[107] Liu W, Wang Z, Wang G, Liu G, Chen J, Pu X, et al. Integrated charge excitation triboelectric nanogenerator. Nat Commun 2019;10(1):1426.
[108] Liu W, Wang Z, Wang G, Zeng Q, He W, Liu L, et al. Switched-capacitor–convertors based on fractal design for output power management of triboelectric nanogenerator. Nat Commun 2020;11(1):1883.
[109] Wang H, Xu L, Bai Y, Wang ZL. Pumping up the charge density of a triboelectric nanogenerator by charge-shuttling. Nat Commun 2020;11(1):4203.
[110] An J, Wang ZM, Jiang T, Liang X, Wang ZL. Whirling-folded triboelectric nanogenerator with high average power for water wave energy harvesting. Adv Funct Mater 2019;29(39):1904867.
[111] Liang X, Jiang T, Feng YW, Lu PJ, An J, Wang ZL. Triboelectric nanogenerator network integrated with charge excitation circuit for effective water wave energy harvesting. Adv Energy Mater 2020;10(40):2002123.
[112] Cheng P, Liu Y, Wen Z, Shao H, Wei A, Xie X, et al. Atmospheric pressure difference driven triboelectric nanogenerator for efficiently harvesting ocean wave energy. Nano Energy 2018;54:156–62.
[113] Kim DY, Kim HS, Kong DS, Choi M, Kim HB, Lee JH, et al. Floating buoy-based triboelectric nanogenerator for an effective vibrational energy harvesting from irregular and random water waves in wild sea. Nano Energy 2018;45:247–54.
[114] Han J, Liu Y, Feng Y, Jiang T, Wang ZL. Achieving a large driving force on triboelectric nanogenerator by wave-driven linkage mechanism for harvesting blue energy toward marine environment monitoring. Adv Energy Mater 2022;13(5):2203219.
[115] Zhou Z, Li X, Wu Y, Zhang H, Lin Z, Meng K, et al. Wireless self-powered sensor networks driven by triboelectric nanogenerator for *in-situ* real time survey of environmental monitoring. Nano Energy 2018;53:501–7.
[116] Li X, Tao J, Wang X, Zhu J, Pan C, Wang ZL. Networks of high performance triboelectric nanogenerators based on liquid–solid interface contact electrification for harvesting low-frequency blue energy. Adv Energy Mater 2018;8(21):1800705.
[117] Chen BD, Tang W, He C, Deng CR, Yang LJ, Zhu LP, et al. Water wave energy harvesting and self-powered liquid–surface fluctuation sensing based on bionic-jellyfish triboelectric nanogenerator. Mater Today 2018;21(1):88–97.
[118] Zhao XJ, Kuang SY, Wang ZL, Zhu G. Highly adaptive solid-liquid interfacing triboelectric nanogenerator for harvesting diverse water wave energy. ACS Nano 2018;12(5):4280–5.
[119] Hong H, Yang X, Cui H, Zheng D, Wen H, Huang R, et al. Self-powered seesaw structured spherical buoys based on a hybrid triboelectric–electromagnetic nanogenerator for sea surface wireless positioning. Energy Environ Sci 2022;15(2):621–32.
[120] Wang H, Zhu Q, Ding Z, Li Z, Zheng H, Fu J, et al. A fully-packaged ship-shaped hybrid nanogenerator for blue energy harvesting toward seawater self-desalination and self-powered positioning. Nano Energy 2019;57:616–24.
[121] Chen H, Wang J, Ning A. Optimization of a rolling triboelectric nanogenerator based on the nano–micro structure for ocean environmental monitoring. ACS Omega 2021;6(32):21059–65.
[122] Xu L, Tang Y, Zhang C, Liu F, Chen J, Xuan W, et al. Fully self-powered instantaneous wireless liquid level sensor system based on triboelectric nanogenerator. Nano Res 2022;15(6):5425–34.
[123] Wang P, Zhang S, Zhang L, Wang L, Xue H, Wang ZL. Non-contact and liquid–liquid interfacing triboelectric nanogenerator for self-powered water/liquid level sensing. Nano Energy 2020;72:104703.
[124] Pang H, Feng Y, An J, Chen P, Han J, Jiang T, et al. Segmented swing-structured fur-based triboelectric nanogenerator for harvesting blue energy toward marine environmental applications. Adv Funct Mater 2021;31(47):2106398.
[125] Feng Y, Han J, Xu M, Liang X, Jiang T, Li H, et al. Blue energy for green hydrogen fuel: a self-powered electrochemical conversion system driven by triboelectric nanogenerators. Adv Energy Mater 2022;12(1):2103143.
[126] Liu X, Xu X, Zhang F, Ge X, Ji H, Li Y, et al. A synergistic anti-corrosion system based on durable superhydrophobic F-SiO_2 /epoxy coatings and self-powered cathodic protection. J Mater Chem A Mater Energy Sustain 2022;10(36):18616–25.
[127] Zhang B, Zhang C, Yuan W, Yang O, Liu Y, He L, et al. Highly stable and eco-friendly marine self-charging power systems composed of conductive polymer supercapacitors with seawater as an electrolyte. ACS Appl Mater Interfaces 2022;14(7):9046–56.